Mixed sneutrinos, dark matter, and the CERN LHC

Zoe Thomas and David Tucker-Smith
Department of Physics, Williams College, Williamstown, Massachusetts 01267, USA

Neal Weiner
Center for Cosmology and Particle Physics, Department of Physics, New York University, New York, New York 10003, USA
(Received 4 January 2008; published 18 June 2008)

We study the phenomenology of supersymmetric models in which gauge-singlet scalars mix with the minimal supersymmetric standard model (MSSM) sneutrinos through weak-scale A terms. After reviewing the constraints on mixed-sneutrino dark matter from measurements of Ω_{CDM} and from direct-detection experiments, we explore mixed-sneutrino signatures relevant to the LHC. For a mixed-sneutrino lightest supersymmetric particle (LSP) and a right-handed slepton next-to-lightest supersymmetric particle (NLSP), decays of the lightest neturalino can produce opposite-sign, same-flavor (OSSF) dileptons with an invariant-mass distribution shifted away from the kinematic end point. This signature is possible for parameters that lead to a cosmologically viable mixed-sneutrino LSP. We also consider signatures that require larger mixing angles than preferred for mixed-sneutrino dark matter, but which are possible regardless of whether a mixed-sneutrino is the LSP. In some parameter regions, the charginos and neutralinos produced in cascades all decay dominantly to the lighter sneutrinos, leading to a kinematic edge in the jet-lepton invariant-mass distribution from the decay chain $\tilde{q} \rightarrow \chi^- q \rightarrow \tilde{\nu}^* l q$, without an OSSF dilepton signature. We explore the possibility of using mass-estimation methods to distinguish this mixed-sneutrino jet-lepton signature from an MSSM one. Finally, we consider signatures associated with Higgs-lepton or Z-lepton production in cascades involving the heavier sneutrinos.

DOI: 10.1103/PhysRevD.77.115015 PACS numbers: 12.60.Jv, 95.35.+d

I. INTRODUCTION

The overwhelming evidence that the majority of the matter in the Universe is nonbaryonic compels us to consider extensions of the standard model which include new fields that are electrically neutral. As was pointed out by Goodman and Witten [1] fields at the weak scale naturally yield the appropriate relic abundance to explain the observed density of dark matter in the Universe. Taken alone, this may be the strongest motivation for new physics at the weak scale.

A second element of physics beyond the standard model that has become firmly established in recent years is neutrino mass. Although it is usually assumed that neutrino mass is generated at very short distances, thus explaining its smallness through the seesaw mechanism [2,3], this hypothesis remains untested, motivating us to consider alternative possibilities.

For example, in supersymmetric theories with right-handed neutrinos at or below the weak scale, small Dirac neutrino masses can be generated as a supersymmetry-breaking effect, or else small Majorana neutrino masses can be generated radiatively or through a weak-scale seesaw [4–6]. Moreover, if the scalar partners of the right-handed neutrinos mix appreciably with the MSSM sneutrinos, the lightest ''mixed'' sneutrino can be considerably lighter than the Z boson [4,6,7], and can also be a viable dark matter candidate [4].

The existence of new states beyond those of the minimal supersymmetric standard model (MSSM) may be crucial for searches at the LHC. Unlike in previous experiments, new particles are likely to be produced in bunches in potentially long cascades. The presence of new states in the cascade chains can lead to new signatures and remove expected ones. It is an intriguing and important question to what extent analyses that can be performed at the LHC might give some indication that a mixed sneutrino is present in the spectrum of the theory.

In this paper we study the cosmology and potential LHC signatures associated with mixed sneutrinos. In Sec. II, we consider the possibility of mixed-sneutrino dark matter, calculating the relic abundance for a range in parameters, and imposing all present constraints from direct-detection experiments, including the most recent from XENON [8]. In agreement with [9], we find that mixed-sneutrino dark matter is viable over substantial parameters regions. We consider the extent to which lepton-number violation in the sneutrino mass matrix might suppress rates at direct-detection experiments, and discuss the connection to neutrino masses.

In Sec. III we explore the collider phenomenology of mixed sneutrinos. The first signature we consider, which persists even for very small sneutrino mixing angles, arises from leptonic decays of the lightest neutralino in the case where the lightest supersymmetric particle (LSP) is the lightest sneutrino and the next-to-lightest supersymmetric particle (NLSP) is a right-handed slepton. The possibility of lepton production from the decays of the lightest neutralino was also pointed out in Ref. [10], which studied the phenomenology of a sneutrino NLSP with a gravitino LSP.

 © 2008 The American Physical Society

We study the invariant-mass distribution of opposite-sign, same-flavor dileptons from these decays and find that it is shifted away from the kinematic end point. The other signatures we consider require somewhat larger mixing angles, as they involve decays of non-NLSP superpartners straight to the lightest sneutrino. For example, in a broad region of parameter space, the gauginos produced in cascades decay almost exclusively directly to the lightest sneutrinos. In this case one has a kinematic edge in the lepton-jet invariant-mass distribution, without a corresponding dilepton edge. We discuss the possibility of distinguishing this signature from MSSM ones, for example, by using recently proposed methods to estimate the masses involved in cascade decays. Finally, we consider signatures from Higgs-lepton or Z-lepton production in cascades involving the heavier sneutrinos, which can lead to distinctive bbl, $\gamma\gamma l$, or trilepton invariant-mass distributions.

II. MIXED-SNEUTRINO DARK MATTER

To be viable, WIMP dark matter candidates must pass three essential tests. First, they must be neutral, both to allow early growth of structure and to have evaded detection. Second, their relic abundance must match the measured value of the dark matter energy density, $\Omega_{\rm CDM}h^2 \sim 0.1$ [11]. Third, given the appropriate relic density they must evade direct-detection experimental limits, the most severe of which presently come from XENON [8] and CDMS [12].

The sneutrino was long ago considered an intriguing dark matter candidate [13,14], but is no longer viable as it fails the combined relic abundance and direct-detection requirements. In particular, a light sneutrino with the appropriate relic abundance would significantly modify the invisible Z-width, in conflict with observation. A heavy sneutrino must be of the order 600 GeV to achieve the correct relic abundance [15], and even then is in clear conflict with direct-detection experiments. Similarly, even if a moderate-mass (~ 100 GeV) sneutrino had come out with the correct relic abundance, it would have been seen at experiments such as CDMS and XENON. One proposal for saving sneutrino dark matter is to suppress coannihilation of the sneutrino's scalar and pseudoscalar components by making them nondegenerate [16], which also eliminates direct-detection constraints arising from Z-exchange contributions to the scattering of sneutrinos off of nuclei. Unfortunately, this scenario implies a ν_τ mass well above the experimental limit.

The problems with sneutrino dark matter mainly stem from the large coupling of sneutrinos to Z bosons. However, because the sneutrino is neutral under electromagnetism, it is free to mix with any additional neutral scalar field, assuming that the field carries lepton number or that lepton number is not a good symmetry of the low-energy theory. This possibility was explored in [4,6,7]. The mixing suppresses the coupling of the lightest sneutrino to the Z, and its mass is allowed to be less than $m_Z/2$ for mixing angles satisfying $\sin\theta \lesssim 0.4$. Because the sneutrino annihilation rate in the early universe is also suppressed, the appropriate relic abundance can be achieved [4].

Related scenarios for sneutrino dark matter include nonthermal right-handed-sneutrino dark matter (where the mixing is extremely tiny) [17,18], and thermally produced right-handed-sneutrino dark matter in the presence of an extra $U(1)$ [19]. The collider phenomenology of the former scenario has been explored in [20,21].

The outline for the rest of the section is as follows. First, we review models of mixed-sneutrino dark matter. Then we discuss the relic abundance calculation and identify cosmologically preferred parameter regions. With these results in mind, we review constraints from direct-detection experiments, and find, in agreement with [9], that significant regions of parameter space remain viable. Lepton-number violation in the sneutrino mass matrix can suppress the scattering of sneutrinos off of nuclei, and thus direct-detection rates, but it also radiatively generates neutrino masses that tend to be beyond experimental limits. We discuss a few scenarios in which these neutrino masses are not problematic, and then briefly consider the implications of sneutrino dark matter for neutrino telescope indirect-detection experiments. Finally, we comment on scenarios in which the gravitino is the LSP, with a mixed-sneutrino NLSP.

A. Mixed sneutrinos with large or small Yukawas

The model we consider is quite simple. To the MSSM, we add one or more additional standard model-singlet superfields N_i, with supersymmetry-breaking trilinear couplings of the form $A_{ij}\tilde{n}_i\tilde{l}_j h_u$. Restricting ourselves for the moment to one generation, this leads to a mass matrix of the form

$$M^2_{\tilde{\nu}} = \begin{pmatrix} m_L^2 + \frac{1}{2}m_Z^2\cos 2\beta & A v \sin\beta \\ A v \sin\beta & m^2_{\tilde{n}} \end{pmatrix}, \qquad (1)$$

with mass eigenstates $\tilde{\nu}_1 = \cos\theta\tilde{n}^* - \sin\theta\tilde{\nu}$ and $\tilde{\nu}_2 = \sin\theta\tilde{n}^* + \cos\theta\tilde{\nu}$. Motivated by the possibility of mixed-sneutrino dark matter, we take $\sin^2\theta < 0.5$, so the lighter state is more singlet than active sneutrino. If this lighter state is heavier than $m_Z/2$ there are no immediate constraints on $\sin\theta$, while if it is lighter than $m_Z/2$, the Z-width constraint requires $\sin\theta < 0.4$.

The A terms for the superpartners of the standard model fermions are typically thought to be related to the associated Yukawa couplings. Given the apparent smallness of the neutrino Yukawa couplings, one thus might not expect sizeable mixing between the active and sterile sneutrinos. However, it is possible that bare Yukawa couplings for the neutrinos are forbidden by a $U(1)_n \otimes U(1)_l$ symmetry that acts independently on the singlet and lepton-doublet superfields. If this symmetry is broken only by supersymmetry-

breaking fields, then weak-scale A terms and tiny Yukawa couplings are perfectly compatible.

Moreover, one can instead have large Yukawa couplings and still have massless neutrinos, as we now describe. If the fields N_i come with fields $\bar{N}_i$ which carry opposite lepton-number charge, we can consider the following superpotential:

$$W \supset \lambda N L H_u + m_N N \bar{N}. \tag{2}$$

When the Higgs acquires an expectation value, there are Dirac masses between ν and n, as well as between n and $\bar{n}$. Because of the mismatch between states with lepton number $+1$ and -1, there is a massless state in the theory. This is essentially the same mechanism that keeps the neutrino light in the standard model. If $m_N > \lambda v_u$ the massless state will then be mostly standard model-neutrino. Constraints on this scenario come from a variety of precision electroweak measurements, principally from measurements of the couplings of charged leptons to neutrinos. For light ($m_N \lesssim m_Z$) neutrinos, λv should be smaller than about m_τ. However, for heavier neutrinos, a larger Yukawa is allowed, even for much lighter sneutrinos. This setup results in a 3×3 sneutrino mass matrix instead of the 2×2 one of Eq. (1),

$$\begin{pmatrix} m_L^2 + \frac{1}{2} m_Z^2 \cos 2\beta & A v \sin\beta + \lambda \mu v \cot\beta & \lambda m_N v \tan\beta \\ A v \sin\beta + \lambda \mu v \cot\beta & m_{\bar{n}}^2 & 0 \\ \lambda m_N v \tan\beta & 0 & \bar{m}_{\bar{n}}^2 \end{pmatrix}. \tag{3}$$

In the limit where m_N (and thus $\bar{m}_{\bar{n}}^2$) are very large, the effective mass matrix for the lighter sneutrinos is the same as in Eq. (1) except with the replacement $A \to X$, where $X = A + \lambda \mu \cot\beta$.

In this setup, nonzero neutrino mass can be generated through higher-dimension operators, or radiatively if small lepton-number-violating terms appear in the full sneutrino mass matrix. For our calculations of direct-detection rates and relic abundances we will restrict ourselves to the model with negligible Yukawa couplings, and leave a thorough analysis of the relic abundance of the Yukawa model to future work. However, it is worth noting that even within the mixed-sneutrino framework, there is great room for variation.

B. Relic abundance of mixed sneutrinos

The dominant annihilation channels for mixed-sneutrinos in the early universe are shown in Fig. 1. These include s-channel Z exchange, t-channel neutralino exchange (to $\nu\nu$ or $\nu\bar{\nu}$), and s-channel Higgs exchange (to fermions, or, for heavier sneutrinos, to gauge bosons and Higgs bosons). The contribution from Higgs exchange is enhanced by the large A-terms, and is often dominant.

To calculate the relic abundance of the mixed-sneutrino LSP, we use the micrOMEGAs 2.0 code [22] with the MSSM model files modified to incorporate the mixed sneutrino. Superpartner and Higgs particle spectra are calculated using SuSpect [23]. We assume that only a single mixed sneutrino has a significant relic abundance today. Even if multiple right-handed sneutrinos are appreciably mixed with the active ones, this will still be true provided the light sneutrinos are not highly degenerate.

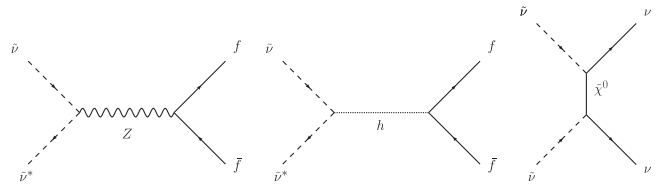

FIG. 1. Diagrams contributing to the mixed-sneutrino annihilation rate in the early universe.

In our calculations we fix the values of the MSSM parameters at the weak scale. We take the input parameters in the sneutrino sector to be the mixing angle θ, the LSP mass $m_{\tilde{\nu}_1}$, and the soft mass-squared for the left-handed sleptons, m_L^2. Once θ and $m_{\tilde{\nu}_1}$ are fixed, both the relic abundance and direct-detection rate (discussed in the following section) are both quite sensitive to m_L^2. This is because increasing m_L^2 increases the A (or X)-parameter, thereby enhancing the annihilation rate via s-channel Higgs exchange and the cross section for Higgs-mediated $\tilde{\nu}_1$-nucleon scattering. The gaugino masses M_1 and M_2 can also be important in determining the relic abundance, as t-channel neutralino exchange is another potentially significant annihilation channel for $\tilde{\nu}_1$.

In Fig. 2 we display regions in $m_{\tilde{\nu}_1}$- $\sin\theta$ space that yield a relic abundance consistent with cosmological observations, for various values of M_1, M_2, and m_L^2. The other MSSM parameters are fixed as $\mu = 300$ GeV, $\tan\beta = 10$, $m_A = 500$ GeV, $m_{l_R} = (300\ \text{GeV})^2$, $m_Q^2 = m_{u_R}^2 = m_{d_R}^2 = M_3 = (1\ \text{TeV})^2$, and $A_t = -1$ TeV, giving a Higgs mass of 116 GeV. Also shown are the constraints from the measurement of the invisible width of the Z and from the recent results from the Xenon10 direct-detection experiment [8].

Let us consider the plots of Fig. 2. In plots (a)–(c), M_1 and M_2 are held fixed as three different values of m_L are used. Importantly, there are dramatic differences in the direct-detection constraints depending on whether elastic scattering via Z-exchange is suppressed—in which case Higgs exchange dominates—or unsuppressed. We will discuss the circumstances in which the Z-exchange contribution is suppressed in the next section.

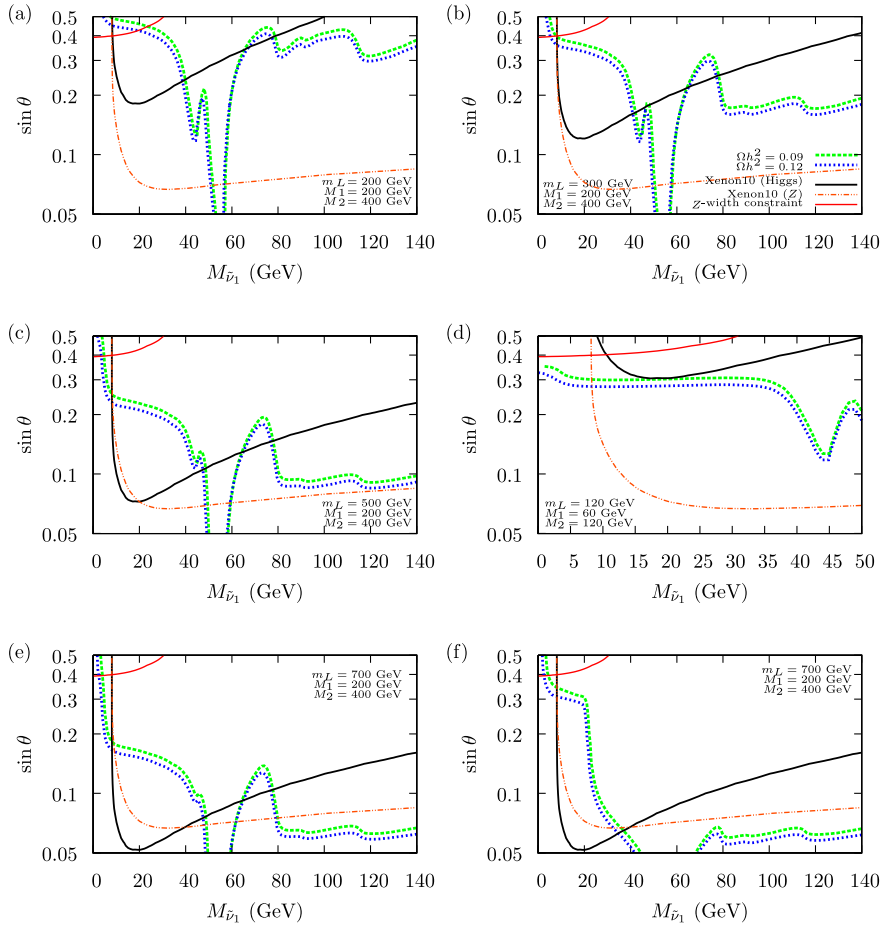

FIG. 2 (color online). Constraints on the sneutrino parameter space from requiring the correct relic abundance, from direct-detection experiments, and from the invisible Z-width measurement. The regions below the Z-width and direct-detection contours are allowed. The values taken for m_L^2, M_1, and M_2 are indicated in the plots, and the other MSSM parameters are as given in the text.

If the Higgs-exchange contribution dominates, we see in (a)–(c) that $\tilde{\nu}_1$ masses above the threshold for W^+W^- production and near the Z or Higgs poles are consistent with what we have learned about the dark matter abundance and with the latest Xenon10 results. As m_L is increased, the interesting regions in parameters space shift to smaller values of $\sin\theta$. If instead the scattering via Z-exchange is unsuppressed, only the Higgs pole region is viable.

In (d) we focus on a particularly light spectrum (both for sneutrinos and gauginos). In this case one sees that without the Z-exchange contribution, sneutrinos with the appropriate relic abundance are allowed over the entire mass range. With unsuppressed Z-exchange scattering, one is forced into the light mass range ($m_{\tilde{\nu}} \lesssim 10$ GeV). The precise mass below which this scenario is viable is not entirely certain, as the issue is sensitive to the highest velocity particles in the halo, for which a modified Gaussian is probably not a good description.

In (e), we take m_L to be very large. As a consequence, there is a large A-term for the same value of $\sin\theta$, making the s-channel Higgs annihilation more efficient, and allowing reasonable relic abundances for low values of $\sin\theta$. Consequently, a broad range of masses is viable, regardless of whether the scattering off of nuclei is dominated by Z or Higgs exchange.

Finally, in (f), we consider the effect of modifying the width of the Higgs. In various recent proposals [24–30], the Higgs width is dominated by final states other than $b\bar{b}$. This possibility is motivated by the fine-tuning problem associated with raising the Higgs mass above the LEP limit. For our purposes, the importance of nonstandard Higgs decays is that they can modify the form of the Higgs pole. We illustrate this by increasing the Yukawa coupling of the b-quark by a factor of 5. One can see that this modification significantly impacts the allowed ranges for mixed-sneutrino dark matter—comparing (e) and (f), the mass ranges from 40–50 GeV and 60–80 GeV open up. It is worth emphasizing that the uncertainties regarding the decays of the Higgs can have significant consequences for the allowed parameter space of any dark matter model which involves annihilation through an s-channel Higgs.

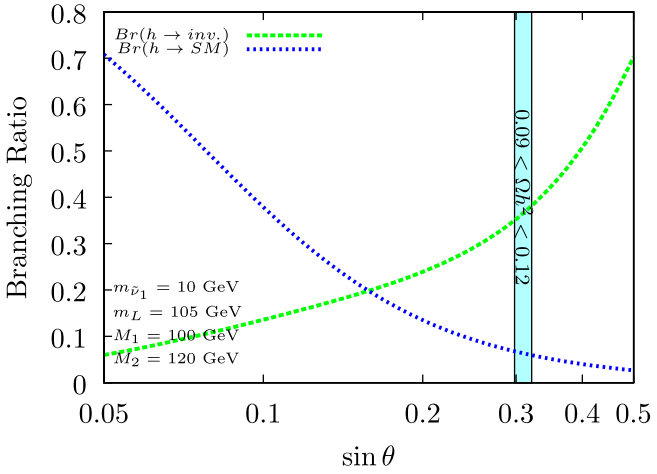

FIG. 3 (color online). Branching ratios for Higgs decays directly to standard model states, and to invisible final states via either $\tilde{\nu}_1\tilde{\nu}_1^*$ or $\tilde{\nu}_1\tilde{\nu}_2$, for the parameters indicated.

It is interesting to note that for the parameters used for Fig. 2(d), with $m_{\tilde{\nu}_1} \sim 10$ GeV and $\sin\theta$ chosen to give the preferred dark matter abundance, the lightest Higgs boson decays invisibly, to $\tilde{\nu}_1\tilde{\nu}_1^*$, more than 80% of the time. If m_L is lowered further, the Higgs also develops an appreciable branching ratio into $\tilde{\nu}_1\tilde{\nu}_2$ final states. Depending on the spectrum—for example, on whether decays to χ_1^0 are accessible— $\tilde{\nu}_2$ may decay dominantly to $\tilde{\nu}_1 Z^*$. In this case, Higgs decays to $\tilde{\nu}_1\tilde{\nu}_2$ would most often produce a rather nondescript final state, although 20% of the time the Z^* would decay to neutrinos, giving an additional contribution to the invisible width of the Higgs. In Fig. 3, we take $Br(\tilde{\nu}_2 \to \tilde{\nu}_1 Z^*) = 100\%$, $m_L = 105$ GeV, and $m_{\tilde{\nu}_1} = 10$ GeV, and plot the branching ratios for a 116 GeV Higgs to decay (i) invisibly and (ii) directly to standard model states, as functions of $\sin\theta$. These branching ratios do not sum to unity because they exclude Higgs decays to $\tilde{\nu}_1\tilde{\nu}_2$ with $\tilde{\nu}_2$ decaying visibly. In fact, we see that for the masses chosen for Fig. 3, and for the values of $\sin\theta$ preferred by cosmology, this third class of decays dominates.

C. Direct and indirect detection of mixed sneutrinos

Cryogenic detectors such as CDMS and liquid noble gas detectors such as XENON have made considerable strides since mixed sneutrinos were originally considered. In this section we consider the cross section for $\tilde{\nu}_1$-nucleon scattering, paying particular attention to the assumptions built in. As indicated in the previous section, we find, consistent with [9], that broad parameter regions remain viable for mixed-sneutrino dark matter, and that broader regions open up in the lepton-number violating case.

Including only the Z-exchange contribution, the cross section for $\tilde{\nu}_1$ to scatter off of nuclei is

$$\sigma = \frac{G_F^2}{2\pi}\mu^2[(A-Z) - (1-4\sin^2\theta_W)Z]^2\sin^4\theta, \qquad (4)$$

where μ is the $\tilde{\nu}_1$-nucleus reduced mass. As discussed above, this cross section exceeds experimental limits for most parameters ranges, with exceptions at small $m_{\tilde{\nu}_1}$, near the Higgs pole, or with heavy left-handed sneutrinos.

Lepton-number violation in the sneutrino mass matrix lifts mass degeneracy between the scalar and pseudoscalar components of the lightest sneutrino, and scattering via Z-exchange occurs inelastically (i.e., through a transition from the scalar to the pseudoscalar or vice versa) [16,31,32]. As a consequence, particles with velocities below

$$\beta_{\min} = \sqrt{\frac{1}{2M_N E_R}}\left(\frac{M_N E_R}{\mu} + \delta\right) \qquad (5)$$

are incapable of scattering. Here, M_N and E_R are the target nucleus mass and recoil energy, and δ is the mass splitting between the scalar and pseudoscalar. Given that there are not expected to be any particles in the halo with velocities above the galactic escape velocity,[1] by dialing δ large (of order 100 keV), one can evade all direct-detection constraints.

In this case, scattering from Higgs exchange still constrains the theory [4]. In the decoupling limit ($m_A \gg m_h$), the cross section for Higgs-mediated $\tilde{\nu}_1$-nucleon scattering is

$$\sigma = \frac{g_{hNN}^2}{4\pi}\left(\frac{g_{h\tilde{\nu}_1\tilde{\nu}_1}}{m_N + m_{\tilde{\nu}_1}}\right)^2\frac{m_N^2}{m_h^4}, \qquad (6)$$

where m_N is the nucleon mass, g_{hNN} is the Higgs-nucleon coupling, and $g_{h\tilde{\nu}_1\tilde{\nu}_1}$ is the coupling of the light Higgs boson to the LSP sneutrino,

$$g_{h\tilde{\nu}_1\tilde{\nu}_1} = -\frac{m_Z^2}{v}\cos 2\beta\sin^2\theta + \frac{A}{\sqrt{2}}\sin\beta\sin 2\theta. \qquad (7)$$

The value of g_{hNN} is subject to rather large uncertainties. Here we adopt the up and down quark, strange quark, and heavy quark contributions to this coupling given in Refs. [33–35], respectively. This yields $g_{hNN} = 1.26 \times 10^{-3}$. Written in terms of this reference value, the cross section is

$$\sigma = \left(\frac{g_{hNN}}{1.26\times10^{-3}}\right)^2\left(\frac{g_{h\tilde{\nu}_1\tilde{\nu}_1}}{m_N + m_{\tilde{\nu}_1}}\right)^2\left(\frac{115\text{ GeV}}{m_h}\right)^4 \times (2.48\times10^{-43}\text{ cm}^2). \qquad (8)$$

1. Relation to neutrino mass

In the lepton-number-violating case gaugino loops generate neutrino masses [5,6]. In the regime in which the diagram with a pure Wino running in the loop dominates,

[1]Or, in our reference frame, $v_{\rm esc} + v_{\rm rot}$, where $v_{\rm rot}$ is the net total velocity from motion of the Earth about the sun, and of the sun about the galactic center.

the correction to the neutrino mass is

$$m_\nu = \frac{g^2 \sin^2\theta \delta m_1 m_2}{32\pi^2} \sum_{ij} f_{ij}, \tag{9}$$

where

$$f_{ij} = \frac{m_{\tilde{W}}^2 m_i^2 \log[m_{\tilde{W}}^2/m_i^2] + m_j^2 m_i^2 \log[m_i^2/m_j^2] + m_{\tilde{W}}^2 m_j^2 \log[m_j^2/m_{\tilde{W}}^2]}{(m_{\tilde{W}}^2 - m_i^2)(m_{\tilde{W}}^2 - m_j^2)(m_i^2 - m_j^2)}, \tag{10}$$

$m_{1,2}$ are the masses of the light and heavy complex eigenstates, and δ is the splitting between the scalar and pseudoscalar components of $\tilde{\nu}_1$.

For much of the parameter space, a splitting of order 100 keV is necessary to ensure that inelastic scattering at XENON is kinematically impossible. With the large mixings (and thus large A-terms) necessary to achieve the appropriate relic abundance, this mass splitting generates a neutrino mass of order 1 eV. Combined with the limits on neutrino mass from cosmology [36], which are roughly 1 eV for the *sum* of the neutrino mass this possibility seems excluded. This has been emphasized recently by [9]. In particular, the authors of [9] argue that inelasticity consistent with neutrino-mass bounds change the allowed parameter space very little. Here we review some important caveats to this.

One point is that the standard value used for galactic escape velocity, 650 km/s, may be too large. Indeed, the most recent simulations of Milky Way type galaxies [37] produce lower escape velocities (~ 450 km/s). Using the distributions of these simulations, rather than the much older halo parameters typically used to set limits, the allowed parameter regions for mixed-sneutrino dark matter do expand. For example, the parameters $m_{\tilde{\nu}_1} = 100$ GeV, $\sin\theta = 0.18$, $m_L = 300$ GeV, $M_2 = 400$ GeV, and $\delta = 50$ keV give a realistic relic abundance and a direct-detection rate that is borderline at XENON, but only generate a neutrino mass of 0.32 eV. Although this mass pushes up against the cosmological limits, this example illustrates how the impact of δ on direct-detection rates is highly sensitive to assumptions about the halo.

A second point is that the radiatively generated neutrino mass is suppressed as the neutralino masses are increased, whereas the $\tilde{\nu}_1$ annihilation rate is insensitive to these masses if it is dominated by s-channel Higgs exchange. For example, for the same parameters as in the previous paragraph, raising M_2 to 1 TeV does not change the relic abundance significantly, but does reduce the neutrino mass to 0.15 eV.

Another possibility is that there might be an enhanced annihilation rate at smaller values of $\sin\theta$. For example, if the neutrino Yukawa couplings are large, as described in Sec. II A, there are additional contributions to the annihilation rate coming from the $\tilde{\nu}_1 \tilde{\nu}_1 h$ coupling $2\lambda^2 v \cos^2\theta$. As this coupling can be parametrically comparable to $A \sin 2\theta$, the annihilation via s-channel Higgs can be considerably enhanced, even at smaller mixing angles. As previously discussed, we leave the analysis of the model with large neutrino Yukawa couplings for future work.

Finally, the neutrino mass of Eq. (9) requires a Majorana mass insertion. If the gauginos are Dirac, as described in [38], a radiative mass will not be generated. In these scenarios, one can disregard the radiative neutrino mass entirely, even for large δ.

When we consider the collider signatures of mixed sneutrinos, some of the parameter points we will study can accommodate mixed-sneutrino dark matter only if the scattering via Z exhange is strongly suppressed, possibly leading to a radiative neutrino mass that is too large. Our main motivation for studying these parameter points is that LHC signatures for mixed sneutrinos are of interest in their own right, independent of the connection to dark matter. However, we also believe that because of the myriad astrophysical and particle physics uncertainties, a liberal take on which regions of parameter space may be cosmologically interesting is warranted.

2. Indirect constraints

Indirect-detection experiments can also place important constraints on mixed-sneutrino dark matter; see [9] for a thorough discussion. Here we focus on the scenario in which inelasticity is relevant.

If $\tilde{\nu}_1$ particles are captured by the sun at a large enough rate, high neutrinos produced in their decays can be detected on Earth. We will allow for the possibility that capture via Z exchange is suppressed by the mass splitting between the scalar and pseudoscalar components of $\tilde{\nu}_1$, so that the capture rate is determined by the contribution from Higgs exchange. In this case we find, following [39], that the most stringent bounds from indirect-detection experiments are not competitive with those from direct detection. For example, taking the parameters used for Figs. 2(b), with $m_{\tilde{\nu}_1} = 100$ GeV and $\sin\theta$ chosen to give the desired relic abundance, we find a flux of upward through-going muons that is almost 2 orders of magnitude below the limits given in [40]. With the parameters used for Fig. 2 (d), and taking $m_{\tilde{\nu}_1} = 10$ GeV, the sneutrinos now annihilate directly to neutrinos, but the predicted flux is still around an order of magnitude or more below current limits,

depending on the flavors of neutrinos produced in the annihilations.

As noted earlier, if the Higgs decays principally in non-standard fashion, then annihilation into neutrinos would be similarly suppressed if annihilation occurs through s-channel Higgs, although this certainly depends sensitively on the decay products of the Higgs boson.

D. LSP gravitinos

In supersymmetric theories in general, an intriguing possibility is that the true LSP is the gravitino, but that the lifetime of the NLSP is sufficiently long that the dark matter relic abundance is determined entirely by the freeze-out of the NLSP [41,42]. Typically, the NLSP is imagined to be a stau or neutralino, but a mixed sneutrino could similarly serve as NLSP, decaying harmlessly into neutrino-gravitino. The sneutrino NLSP case was considered within the MSSM in [10].

In this gravitino-LSP scenario the parameter space opens up dramatically, including regions with otherwise too large relic abundance, or regions where the XENON limits would have excluded mixed-sneutrino dark matter. This gives us extra motivation to be open-minded when studying the collider phenomenology of mixed sneutrinos. Unfortunately, this gravitino-LSP scenario leads to no signals at dark matter detectors, either direct or indirect.

III. LHC SIGNATURES

What experimental signatures for mixed sneutrinos might be observed at the LHC? This depends on the superpartner spectrum and, crucially, on the amount of mixing between the sterile and active sneutrinos. In Sec. III A we consider the case where the mixing angle θ is quite small. In this case the mostly sterile sneutrinos will be produced only rarely in cascade decays, unless they are the lightest superpartners. If they *are* the lightest superpartners, they will be produced in the decays of the NLSP, and the collider signatures depend on the identity of that particle. In Sec. III A we will see that if the NLSP is a right-handed slepton, a distinctive opposite-sign dilepton signature potentially emerges. If the NLSP is instead χ_1^0, the collider phenomenology will be the same as with a neutralino LSP, but even in this case, there is a simple point to be made: a given cosmologically disfavored point in MSSM parameters space may become cosmologically viable with a mixed-sneutrino added at the bottom of the spectrum.

In Secs. III B and III C, we consider additional signatures that become possible if the mixing angle is larger, $\theta \gtrsim 0.1$. We have seen that, for these larger mixing angles, there is tension between having the correct relic abundance, evading direct-detection experiments, and satisfying the neutrino-mass bound. While in certain variations of the model this tension may be eliminated (e.g. in a scenario with Dirac gauginos), we regard these mixed-sneutrino signatures as important to study independent of whether the sneutrinos produced are the cold dark matter, for the following reasons:

(i) Discovering mixed-sneutrinos at the LHC would shed important light on the nature of neutrino masses; it would suggest that the neutrinos are of Dirac type, or else, that the seesaw scale is not much larger than the weak scale.

(ii) Even if the sneutrinos produced at the LHC are not the dark matter, they could still be relevant to the dark matter question. Here are two possible scenarios that illustrate this point: (1) The lightest mixed sneutrino is the NLSP. It freezes out in the early universe and then decays to gravitino dark matter. (2) In addition to the sneutrinos with large enough mixing angles to be produced at the LHC, there is a lighter one with a smaller active component, suitable to be the cold dark matter.

In Sec. III B we consider kinematic edges that can appear in jet-lepton invariant-mass distributions when charginos decay directly to mixed sneutrinos. We also discuss the possibility of using mass-estimation techniques to distinguish this signature from MSSM ones. In Sec. III C we study signatures associated with decays of the heavier sneutrinos to the lighter ones, involving Higgs and Z bosons.

A. Dilepton mass distributions

Assuming that a mixed sneutrino is the LSP, its presence at the end of every cascade decay chain makes for SUSY signals rich in leptons. In this section, we consider cascades involving a right-handed slepton NSLP, and find the following:

(i) Opposite-sign same-flavor (OSSF) dileptons can arise from a two-body decay followed by a three-body decay, whereas in the MSSM they typically come from two-body followed by two-body, or from a single three-body decay. If the final-state leptons are mostly μ or e, this allows us to distinguish the mixed-sneutrino scenario from the MSSM over significant regions of parameter space.

(ii) If $\tilde{\tau}_1$ is produced, rather than $\tilde{e}_R$ or $\tilde{\mu}_R$, a prominent signal is still possible and may be distinguishable from the MSSM.

If the LSP is a weakly mixed sneutrino and the NLSP is a right-handed slepton, we have the following possible decays for the lightest neutralino:

$$\chi_1^0 \to \tilde{\nu}_1 \nu, \qquad \chi_1^0 \to \tilde{\tau}_1 \tau, \qquad \chi_1^0 \to \tilde{l}_R l, \tag{11}$$

where $l = e, \mu$. The direct decay to $\tilde{\nu}_1 \nu$ is suppressed by the small mixing angle, leaving $\tilde{\tau}_1 \tau$ and $\tilde{l}_R l$ as the competing decay channels. We will assume for now that $\chi_1^0 \to \tilde{l}_R l$ has a substantial branching ratio, and consider the case where $\chi_1^0 \to \tilde{\tau}_1 \tau$ completely dominates at the end of this section.

Under this assumption, we expect a large number of right-handed sleptons to be produced at the LHC. How do they decay? The possibilities are

$$\tilde{l}_R \to \tilde{\nu}_1 W, \qquad \tilde{l}_R \to \tilde{\tau}_1 \tau l, \qquad \tilde{l}_R \to \tilde{\nu}_1 \nu l. \tag{12}$$

Even if the two-body decay to $\tilde{\nu}_1 W$ is kinematically accessible, it is not only suppressed by the sneutrino mixing angle, but also vanishes in the absence of left-right slepton mixing. For $\theta \sim 0.05$, it is typically negligible compared to the three-body decays for $l = e$, and only potentially competitive for $l = \mu$. Note also that the relevant coupling here depends on flavor issues—if the active component of $\tilde{\nu}_1$ is entirely third generation, these decays are absent. The second decay, to $\tilde{\tau}_1 \tau l$, may or may not be kinematically allowed. Even if it is allowed, its kinematical suppression can easily make the third decay, to $\tilde{\nu}_1 \nu l$, the dominant one. As we will illustrate by example below, this is true even though the decay to $\tilde{\nu}_1 \nu l$ is mixing-suppressed.

Assuming, then, that $\chi_1^0 \to \tilde{l}_R l$ and $\tilde{l}_R \to \tilde{\nu}_1 \nu l$ both have substantial branching ratios, an OSSF dilepton signature results. The $l^+ l^-$ invariant-mass distribution is predicted to have a kinematic end point at

$$m_{l^+l^-}^{\max} = m_{\chi_1^0} \sqrt{1 - (m_{\tilde{l}_R}/m_{\chi_1^0})^2} \sqrt{1 - (m_{\tilde{\nu}_1}/m_{\tilde{l}_R})^2}. \tag{13}$$

In supersymmetric models, OSSF dilepton signatures, with associated kinematic edges, are quite common. How distinctive is the dilepton mass distribution in the case with a mixed-sneutrino LSP?

In standard SUSY models, an OSSF dilepton signature can arise via the sequence of two-body decays $\chi_2^0 \to (\tilde{l}) l^+ \to (\chi_1^0 l^-) l^+$. One important difference compared to this standard case is simply that in the mixed-sneutrino LSP case, the dileptons come from χ_1^0 decays. Provided the relevant branching ratios are sizable we would thus typically expect a larger lepton multiplicity than in the case where χ_2^0 initiates the decays. However, χ_1^0 decays can also produce an OSSF dilepton signature in a scenario with a gravitino LSP and a right-handed slepton NLSP, through the sequence $\tilde{\chi}_1^0 \to (\tilde{l}_R) l^+ \to (\tilde{G} l^-) l^+$ (prompt decays of the NLSP slepton are possible for a low SUSY-breaking scale).

These scenarios are easily distinguished from the mixed-sneutrino case by their dilepton invariant-mass distributions. The two-body/two-body sequences $\chi_2^0 \to (\tilde{l}) l^+ \to (\chi_1^0 l^-) l^+$ and $\tilde{\chi}_1^0 \to (\tilde{l}_R) l^+ \to (\tilde{G} l^-) l^+$ both have the distribution

$$\frac{dP}{dm_{l^+l^-}} \propto m_{l^+l^-}. \tag{14}$$

If we take the matrix element of the three-body decay to be constant and just consider the phase-space dependence, the two-body/three-body sequence $\chi_1^0 \to (\tilde{l}_R) l^+ \to (\tilde{\nu}_1 \nu l^-) l^+$ gives

$$\frac{dP}{dx} \propto x\left(1 - x^2 - \mu^2\left[1 + \ln\left(\frac{1 - x^2}{\mu^2}\right)\right]\right), \tag{15}$$

where we have defined $x = m_{l^+l^-}/\sqrt{m_{\tilde{\chi}_1^0}^2 - m_{\tilde{l}_R}^2}$, $\nu = m_{\tilde{l}_R}/m_{\tilde{\chi}_1^0}$, and $\mu = m_{\tilde{\nu}}/m_{\tilde{l}_R}$. Normalized plots of these very different looking distributions are shown in Fig. 4.

A softer dilepton invariant-mass distribution arises in the MSSM if the leptons come from a three-body decay such as $\chi_2^0 \to \chi_1^0 l^+ l^-$. In this case the end point of the distribution is just the mass difference between two neutralinos,

$$m_{l^+l^-}^{\max} = m_{\chi_2^0} - m_{\chi_1^0}. \tag{16}$$

Again taking the matrix element of the three-body decay to be constant and considering the phase-space dependence alone, the dilepton invariant-mass distribution is

$$\frac{dP}{dx} \propto x\sqrt{(1 - x^2)((1 - K^2)^2 - x^2)}, \tag{17}$$

where $x = m_{l^+l^-}/(m_{\tilde{\chi}_2^0} - m_{\tilde{\chi}_1^0})$ and $K = 2m_{\tilde{\chi}_1^0}/(m_{\tilde{\chi}_2^0} - m_{\tilde{\chi}_1^0})$. In the massless-LSP limit, this distribution and the two-body/three-body distribution of Eq. (15) both reduce to

$$\frac{dP}{dx} \propto x(1 - x^2), \tag{18}$$

where $x = m_{l^+l^-}/m_{l^+l^-}^{\max}$. Although these distributions are identical in the massless-LSP limit, they shift in opposite directions as the LSP mass increases, as shown in Fig. 5. There we see that the mixed-sneutrino distributions are significantly softer than what the MSSM three-body decays give, unless the LSP neutralino mass for the MSSM case is unusually small. Other observables, such as the overall lepton multiplicity, would likely help to further

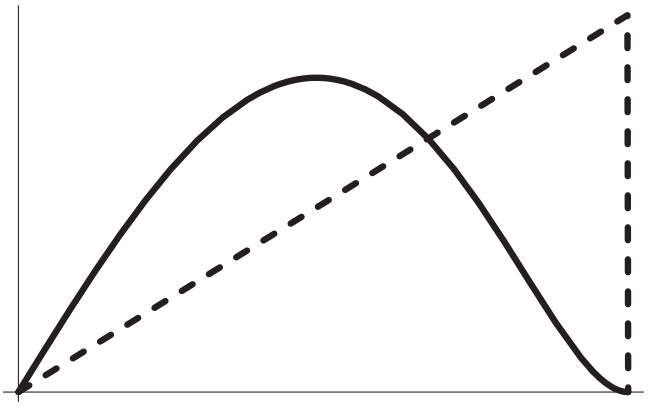

FIG. 4. OSSF dilepton invariant-mass distributions from the sequence of two-body decays $\chi_2^0 \to (\tilde{l}) l^+ \to (\chi_1^0 l^-) l^+$ (dashed line), and from the two-body/three-body sequence $\chi_1^0 \to (\tilde{l}_R) l^+ \to (\tilde{\nu}_1 \nu l^-) l^+$ (solid line). For the latter, the amplitude of the three-body decay is set to be constant, and we take $m_{\tilde{l}_R} = 0.8 m_{\tilde{\chi}_1^0}$ and $m_{\tilde{\nu}} = 0.5 m_{\tilde{\chi}_1^0}$.

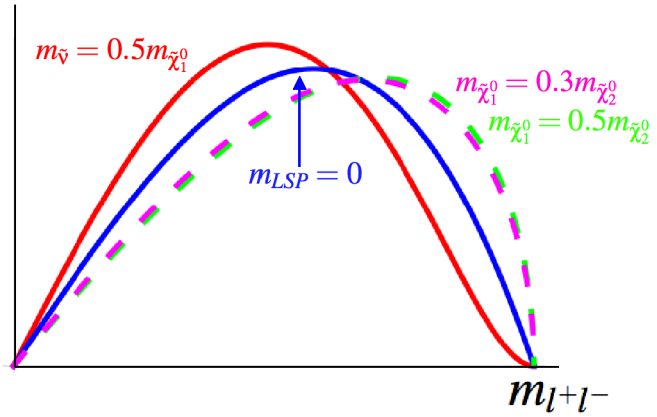

FIG. 5 (color online). OSSF dilepton invariant-mass distributions for the three-body decay $\chi_2^0 \to \chi_1^0 l^+ l^-$ (dashed line), and for the two-body/three-body sequence $\chi_1^0 \to (\tilde{l}_R) l^+ \to (\tilde{\nu}_1 \nu l^-) l^+$ (solid line). For the latter, the amplitude of the three-body decay is set to be constant, and we take $m_{\tilde{l}_R} = 0.8 m_{\tilde{\chi}_1^0}$. The distributions are identical for the massless-LSP case, shown in the middle.

distinguish particular points in the parameter spaces of these two scenarios. Moreover, as we will see, the observed value of the kinematic end point of the $m_{l^+l^-}$ distribution may not be easily reconciled with a very small value of $m_{\tilde{\chi}_1^0}/m_{\tilde{\chi}_2^0}$.

We have used Monte Carlo simulation to explore the distinguishability of these scenarios further. We modified the SUSY-HIT package [43] for calculating superpartner masses and decay branching ratios to incorporate mixed sneutrinos and the associated decays. For example, the three-body decays of right-handed sleptons were implemented by appropriately modifying the matrix elements given for three-body squark decays. We generated events with full SUSY production using Pythia 6.4 [44], with the pytbdy.f file modified to include the momentum dependence in the amplitudes for the three-body decays of right-handed sleptons via off-shell bino,

$$|\mathcal{M}(\tilde{l}_R \to \tilde{\nu}\, \bar{\nu}\, l)|^2 = 4g'^4 m_{\tilde{l}_R}^2 \frac{4E_l E_\nu - m_{l\nu}^2}{(m_{\tilde{\chi}_1^0}^2 - m_{\nu\tilde{\nu}}^2)^2}, \tag{19}$$

$$|\mathcal{M}(\tilde{l}_R \to \tilde{\nu}^* \nu l)|^2 = 4g'^4 \frac{m_{\tilde{\chi}_1^0}^2 m_{l\nu}^2}{(m_{\tilde{\chi}_1^0}^2 - m_{\nu\tilde{\nu}}^2)^2}. \tag{20}$$

Here $m_{l\nu}$ and $m_{\nu\tilde{\nu}}$ are the lepton-neutrino and neutrino-sneutrino invariant masses, respectively. The momentum dependence for three-body neutralino decay amplitudes is already included in Pythia. After generating the fully showered and hadronized Pythia events, we passed these to the PGS 4.0 detector simulator [45], taking the granularity of the calorimeter grid to be $\delta\eta \times \delta\phi = 0.1 \times 0.1$.

For the mixed-sneutrino case, we start with the mSUGRA-like high-scale parameters $\tilde{m}^2 = (10\ \text{GeV})^2$, $M_{1/2} = 450$ GeV, $\tan\beta = 10$, $A_t = -500$ GeV, and $A_b = A_\tau = 0$. Then we add a weakly mixed sneutrino with $\theta = 0.05$ and $m_{\tilde{\nu}_1} = 58$ GeV to the bottom of the resulting spectrum. The physical superpartner masses for this point are given in Table I.

The most important masses for the dilepton signature are $m_{\tilde{\chi}_1^0}$, $m_{\tilde{l}_R}$, and $m_{\tilde{\nu}_1}$, whose values lead to a kinematic end point of $m_{l^+l^-}^{\max} = 63$ GeV. For the parameter point chosen, the branching ratios for the lightest neutralino are $Br(\chi_1^0 \to \tilde{l}_R l) = 41\%$, $Br(\chi_1^0 \to \tilde{\tau}_1 \tau) = 57\%$, and $Br(\chi_1^0 \to \tilde{\nu}_1 \nu) = 2\%$. The branching ratios for the right-handed selectrons are $Br(\tilde{e}_R \to \tilde{\nu}_1 \nu e) = 97\%$ and $Br(\tilde{e}_R \to \tilde{\tau}_1 \tau \nu) = 3\%$, and the branching ratios for the right-handed smuons are $Br(\tilde{\mu}_R \to \tilde{\nu}_1 \nu \mu) = 69\%$, $Br(\tilde{\mu}_R \to \tilde{\nu}_1 W) = 29\%$, and $Br(\tilde{\mu}_R \to \tilde{\tau}_1 \tau \nu) = 2\%$. The total widths for $\tilde{e}_R$ and $\tilde{\mu}_R$ are both hundreds of eV, so we can assume that they decay promptly. Note that although we mix in three generations of sterile sneutrinos, all with the same mixing angle, the detectability of the dilepton signature does not rely on this

TABLE I. Superpartner and Higgs boson masses for the parameter point used to study the dilepton signature in the mixed-sneutrino case. All masses are in GeV.

$m_{\tilde{g}}$	1039
$m_{\tilde{\chi}_2^\pm}$	678
$m_{\tilde{\chi}_1^\pm}$	349
$m_{\tilde{\chi}_4^0}$	678
$m_{\tilde{\chi}_3^0}$	668
$m_{\tilde{\chi}_2^0}$	350
$m_{\tilde{\chi}_1^0}$	184
$m_{\tilde{u}_L}$	948
$m_{\tilde{u}_R}$	915
$m_{\tilde{d}_L}$	952
$m_{\tilde{d}_R}$	912
$m_{\tilde{t}_2}$	914
$m_{\tilde{t}_1}$	663
$m_{\tilde{b}_2}$	910
$m_{\tilde{b}_1}$	860
$m_{\tilde{l}_L}$	303
$m_{\tilde{l}_R}$	172
$m_{\tilde{\tau}_2}$	306
$m_{\tilde{\tau}_1}$	162
$m_{\tilde{\nu}_2}$	293
$m_{\tilde{\nu}_1}$	58
$m_{H^\pm}$	730
m_H	726
m_A	726
m_h	116

simplifying assumption. For example, if there is only a single sterile sneutrino which mixes with the stau sneutrino alone, the branching ratios for $\tilde{\mu}_R \to \tilde{\nu}_1 \nu\mu$ and $\tilde{e}_R \to \tilde{\nu}_1 \nu e$ are both above 90%—the branching ratio actually goes up for $\tilde{\mu}_R$ because it can no longer go to $\tilde{\nu}_1 W$.

For this parameter point, we find using Prospino 2.0 [46] that the NLO cross section for squark and gluino production [47,48] is 2.7 pb. We generate 80 000 events, corresponding to $\sim$30 fb^{-1}. In our analysis, we demand either an e^+e^- pair or a $\mu^+\mu^-$ pair, where the leptons are required to have $p_T > 10$ GeV and $|\eta| < 2.4$. To suppress standard model background, we further require $\sum p_T > 1500$ GeV, where the sum is over jets with $p_T > 20$ GeV, leptons and photons with $p_T > 10$ GeV, and missing p_T. After this cut the leading standard model background is from $t\bar{t}$, which we also simulate using Pythia. We generate 18.9×10^6 $t\bar{t}$ events, corresponding to 23 fb^{-1} of integrated luminosity, where we take $\sigma = 830$ pb for the $t\bar{t}$ production cross section at NLO [49]. After the cuts, we have 850 $t\bar{t}$ events after rescaling to 30 fb^{-1}, compared with 8812 events from SUSY production.

In the first plot of Fig. 6, we show the OSSF dilepton invariant-mass distribution for events passing the cuts. The distribution rapidly decreases as the mass approaches the expected end point $m_{l^+l^-}^{\max} = 63$ GeV from below. It then levels off due to the relatively large SUSY background. This background can be dealt with using a standard flavor subtraction, as shown in the second plot of the same figure. To make that plot, the analysis is redone, this time demanding either an $e^+\mu^-$ pair or a μ^+e^- pair. The opposite-sign dilepton invariant-mass distributions for these events are then subtracted from the OSSF distribution. We see that this procedure does a good job reducing the SUSY background, and the kinematic end point is evident, within a few GeV or so of the expected position at 63 GeV.

A simple modification to this parameter point is to remove the mixed-sneutrino LSP with a light gravitino, with the assumption that $\tilde{e}_R$ and $\tilde{\mu}_R$ decay promptly to it (this will not be the case if decays to $\tilde{\tau}_1$ are accessible). If we adjust the right-handed slepton mass to keep the OSSF dilepton end point near 63 GeV, we find the distribution shown in the first plot of Fig. 7. As expected, the differences compared to the mixed-sneutrino case are clear due to the two-body kinematics of the relevant decays.

We now want to compare the mixed-sneutrino distribution with that from a MSSM parameter point in which the three-body decays $\chi_2^0 \to \chi_1^0 l^+ l^-$ are important. So, we choose low-scale parameters such that the most relevant physical masses are $m_{\tilde{\chi}_1^\pm} = 101$ $m_{\tilde{\chi}_2^0} = 101$ GeV, $m_{\tilde{\chi}_1^0} = 37$ GeV, $m_{\tilde{l}_L} = 129$ GeV, and $m_{\tilde{\nu}} = 102$ GeV. The pa-

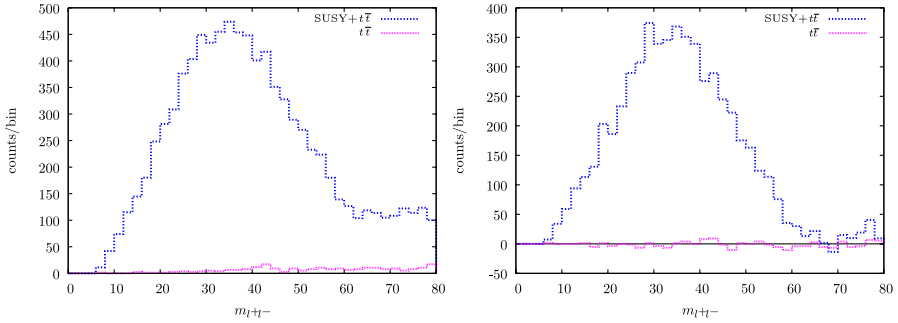

FIG. 6 (color online). Left: OSSF dilepton invariant-mass distributions for SUSY events and $t\bar{t}$ background. Right: flavor-subtracted opposite-sign dilepton invariant-mass distributions.

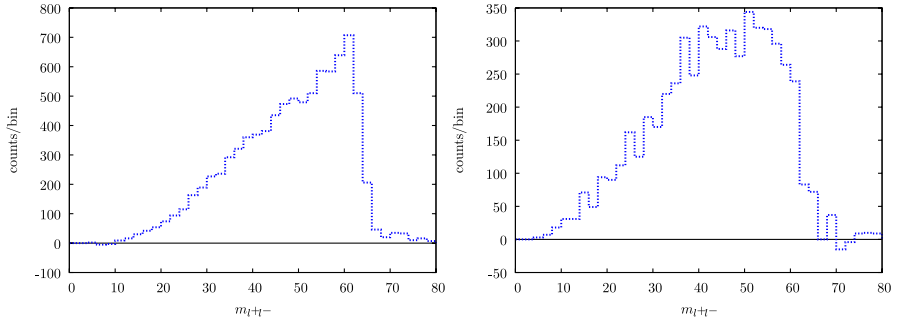

FIG. 7 (color online). Flavor-subtracted OSSF dilepton invariant-mass distributions in (left) the gravitino-LSP case and (right) the MSSM case with the three-body decay $\chi_2^0 \to \chi_1^0 l^+ l^-$.

rameters are chosen so that the splitting between $m_{\tilde{\chi}_2^0}$ and $m_{\tilde{\chi}_1^0}$ gives a kinematic end point very close to the 63 GeV value from the mixed-sneutrino case. Also, the gaugino masses are taken as small as they can be consistent with negative results from direct SUSY searches at LEP. The rationale for doing this is to soften the dilepton invariant-mass distribution as much as possible, to see how similar to the mixed-sneturino distribution it can look (recall that the distributions should be very similar in the massless-LSP limit). Another way to soften the $m_{l^+l^-}$ distribution is to make the intermediate slepton in the three-body decay just barely off shell. So, we make m_L small; however, we want to ensure that the two-body decay $\chi_2^0 \to \tilde{\nu}\nu$ is not kinematically accessible, which prevents us from lowering $m_{\tilde{l}_L}$ arbitrarily close to $m_{\tilde{\chi}_2^0}$. Note that for the parameters chosen $m_{\tilde{\nu}}$ is just above $m_{\tilde{\chi}_2^0}$.

The flavor-subtracted $m_{l^+l^-}$ distribution for this set of parameters is shown in the second plot of Fig. 7. The distribution is softer than in the gravitino-LSP case, but still easily distinguished from the mixed-sneutrino distribution of Fig. 6. Had the value of the kinematic end point for the mixed sneutrino been significantly larger it would presumably allow one to find a point in the MSSM parameter space that gives a more similar looking distribution. For this reason we stress that other observables, such as the overall lepton multiplicity, may also be useful for distinguishing particular points in the two parameter spaces. A detailed study of a number of relevant observables at once would likely be efficient at ruling out candidate parameter points.

For example, for the particular point we have chosen on the mixed-sneutrino side, an additional distinctive feature evident in the $m_{l^+l^-}$ distribution is a second kinematic edge at ~140 GeV. This is shown in Fig. 8, which is essentially a zoomed-in view of Fig. 6, going out to larger invariant masses. The flavor-subtracted distribution does not average to zero beyond ~63 GeV because OSSF dileptons can also come from the two-body/two-body sequence $\chi_2^0 \to (\tilde{l})l^+ \to (\chi_1^0 l^-)l^+$, and the kinematic end point for this sequence is indeed near 140 GeV for the parameters chosen. The possible presence of two edges, one associated with $\tilde{\chi}_2^0$ decays and the other associated $\tilde{\chi}_1^0$ decays, is one more puzzle piece one could use to distinguish points in mixed-sneutrino parameter space from points in MSSM parameter space.

Decays to τ's

We conclude this section by considering the possibility that $\chi_1^0 \to \tilde{\tau}_1\tau$ is the dominant decay of the lightest neutralino, with nearly 100% branching ratio. In this case, the signature involving e^+e^- or $\mu^+\mu^-$ pairs is absent, and the situation becomes more challenging experimentally. If $\tilde{\tau}_1$ decays dominantly to $\tilde{\nu}_1\nu\tau$, then one could hope to observe an end point in the ditau invariant-mass distribution. However, if $\tilde{\tau}_1 \to \tilde{\nu}_1 W$ is kinematically accessible, it is likely to dominate. Here we assume this two-body decay is kinematically accessible and consider the detectability of $\tilde{\chi}_1^0 \to (\tilde{\tau}_1)\tau^+ \to (\tilde{\nu}_1 W^-)\tau^+$, with the W decaying leptonically.

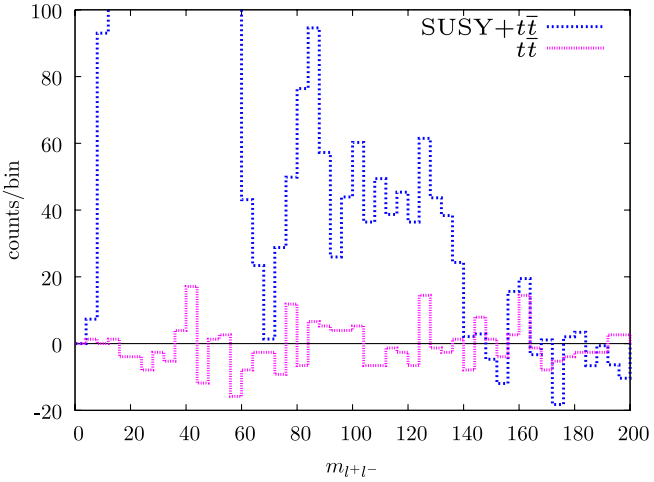

FIG. 8 (color online). Flavor-subtracted OSSF dilepton invariant-mass distributions for SUSY events and $t\bar{t}$ background, in the mixed-sneutrino case. A second kinematic end point is visible at ~140 GeV.

To study this issue we take the high-scale parameters $\tilde{m}^2 = (50\ \text{GeV})^2$, $M_{1/2} = 350$ GeV, $\tan\beta = 10$, $A_t = -500$ GeV, and $A_b = A_\tau = 0$. Then we add a weakly mixed sneutrino with $\theta = 0.05$ and $m_{\tilde{\nu}_1} = 51$ GeV. For the purposes of this study, the most important masses are $m_{\tilde{\chi}_1^0} = 141$ GeV, $m_{\tilde{\tau}_1} = 134$ GeV, and $m_{\tilde{\nu}_1} = 51$ GeV, and the most important branching ratios are $Br(\chi_1^0 \to \tilde{\tau}_1\tau) = 94\%$ and $Br(\tilde{\tau}_1 \to \tilde{\nu}_1 W) = 94\%$. In the sequence $\chi_1^0 \to (\tilde{\tau}_1)\tau^+ \to (\tilde{\nu}_1[W^-])\tau^+ \to (\tilde{\nu}_1[l\bar{\nu}])\tau^+$, the invariant-mass of the final-state lepton and tau has an upper bound of 37 GeV for the masses considered.

We find the total SUSY production cross section for this point to be 10.6 pb for pp collisions at $\sqrt{s} = 14$ TeV, and work with ~587 000 events, corresponding to about 55 fb^{-1} of integrated luminosity. We take all events with at least one reconstructed τ and at least one isolated lepton (e or μ), and as before we apply a cut $\sum p_T > 1500$ GeV to reduce standard model backgrounds. The invariant mass $m_{\tau l}$ is calculated for all τ-lepton pairings with opposite sign, giving the OS $m_{\tau l}$ distribution shown in the first plot of Fig. 9. Repeating the same procedure, this time requiring the τ and the lepton to have the *same* sign, gives the SS distribution in the same plot. The peak at low invariant mass in the OS distribution arises from events with $\chi_1^0 \to (\tilde{\tau}_1)\tau^+ \to (\tilde{\nu}_1[W^-])\tau^+ \to (\tilde{\nu}_1[l\bar{\nu}])\tau^+$. The OS distribution is similar to the SS distribution beyond this peak, but an excess in the OS distribution over the SS distribution does persist beyond the expected 37 GeV end point, because there are other ways to produce opposite-sign leptons and

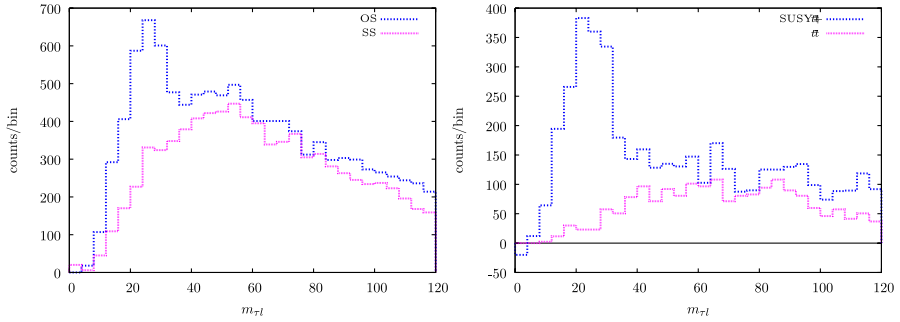

FIG. 9 (color online). Left: opposite-sign (OS) and same-sign (SS) lepton-tau invariant-mass distributions from SUSY production alone. Right: opposite-sign minus same-sign distributions for SUSY plus $t\bar{t}$ production, and for $t\bar{t}$ production alone.

taus in association with each other $(\chi_2^0 \to (\tilde{\tau}_1)\tau^+ \to (\tilde{\nu}_1[W^-])\tau^+ \to (\tilde{\nu}_1[l\bar{\nu}])\tau^+$ being just one example).

To gauge whether this signature would be observable above background, we include the $t\bar{t}$ sample generated with Pythia. Taking the difference between the OS and SS distributions for both the SUSY and $t\bar{t}$ backgrounds, we find the subtracted distributions shown in the second plot of Fig. 9. Despite the significant $t\bar{t}$ and SUSY backgrounds, a rather dramatic fall-off in the distribution is evident for invariant masses between 30 and 40 GeV.

In the MSSM, the decay $\tilde{\nu}_\tau \to \tilde{\tau}_1 W^+$ may occur due to the left-right stau mixing. If the stau subsequently decays as $\tau_1 \to \tilde{\chi}_1^0 \tau$, then we have associated W- τ production, just as we had in the mixed-sneutrino case. Here we do not explore in detail the extent to which this MSSM decay sequence could be distinguished from the mixed-sneutrino decay sequence considered above, but simply note that in the mixed-sneutrino scenario the signal has the potential to be much more prominent, given that it originates from $\tilde{\chi}_1^0$ decays rather than $\tilde{\nu}_\tau$ decays.

B. Jet-lepton mass distributions

At the LHC, most SUSY events will begin with squark or gluino production, and so leptons produced in association with mixed sneutrinos will typically be accompanied by hard jets. In this section, we consider the impact of mixed sneutrinos on jet-lepton invariant-mass distributions, and find the following:

(i) The decay chain $\tilde{q} \to (\chi^\pm)q \to (\tilde{\nu}_1 l)q$ leads to a prominent edge in this distribution, providing a potentially distinctive signature for mixed-sneutrino production.

(ii) A recently proposed mass-estimation method [50] can be used to probe the spectrum of the theory when applied to events involving this decay chain. That method can thus be used to help distinguish mixed-sneutrino and MSSM scenarios, although in our implementation it does not reliably estimate the sneutrino mass.

If the sneutrino mixing angle θ is large enough, then chargino and neutralino decays directly to $\tilde{\nu}_1$ can become important. In fact, it is easy to imagine a situation in which $\chi_2^0 \to \tilde{\nu}_1 \nu$ and $\chi_1^\pm \to \tilde{\nu}_1 l$ both have nearly 100% branching ratios. To illustrate this with a concrete example, we take the high-scale parameters $\tilde{m}^2 = (200\ \text{GeV})^2$, $\tilde{m}^2_{H_u,H,d} = 0$ $M_{1/2} = 300$ GeV, $\tan\beta = 10$, $A_t = -500$ GeV, and $A_b = A_\tau = 0$. We add to the resulting MSSM spectrum mixed sneutrinos with $\theta = 0.2$ and $m_{\tilde{\nu}_1} = 108$ GeV. The superpartner spectrum for these parameters is given in Table II. From this table we see that the only two-body decays available to $\chi_1^\pm$ are to $\tilde{\nu} l$, $\tilde{\chi}_1^0 W$, and $\tilde{\tau}_1 \nu$. The branching ratios for these final states are 95%, 4%, and $<1\%$, respectively. As before, we make the simplifying assumption that all three generations of sterile sneutrinos have equal mixing angles with the active states. If there is only one sterile sneutrino, which only mixes appreciably with $\tilde{\nu}_\tau$, then $\chi^\pm$ will decay almost exclusively to $\tilde{\nu}_1 \tau$. In this case detecting the chargino decays becomes more challenging.

Although $\tilde{\nu}_1$ is lighter than $\tilde{\chi}_1^0$ in the above spectrum, this ordering is not important for the signature we are about to explore. If we had taken $m_{\tilde{\nu}_1} = 140$ GeV instead, we would still have $Br(\chi_1^\pm \to \tilde{\nu} l) = 93\%$. So it is not essential for the following discussion that $\tilde{\nu}_1$ is the LSP. We should also note that, given how dominant $\chi_1^\pm \to \tilde{\nu} l$ is for the parameters we have chosen, that decay mode still easily dominates for more modest values of the mixing angle, $\theta \sim 0.1$. So, signatures associated with $\chi_1^\pm \to \tilde{\nu} l$ can exist for those smaller mixing angles as well.

For the parameters chosen, $\tilde{\chi}_2^0$ also decays dominantly straight to $\tilde{\nu}_1$, with a branching ratio greater than 99%. Because of the presence of $\tilde{\nu}_1$, both $\tilde{\chi}_1^0$ *and* $\tilde{\chi}_2^0$ appear as missing energy in the detector. In particular, although there are leptons produced in chargino decays, there is no OSSF dilepton signal initiated by $\tilde{\chi}_2^0$ decays.

Chargino production via squark decay leads to the following sequence: $\tilde{q} \to (\chi^\pm)q \to (\tilde{\nu}_1 l)q$. One then expects to observe a kinematic end point in the jet-lepton invariant-mass distribution at

$$m_{ql}^{\max} = m_{\tilde{q}} \sqrt{1 - (m_{\chi_1^\pm}/m_{\tilde{q}})^2} \sqrt{1 - (m_{\tilde{\nu}_1}/m_{\chi_1^\pm})^2}. \quad (21)$$

TABLE II. Superpartner and Higgs boson masses for the parameter point used to study the jet-lepton signature. All masses are in GeV.

$m_{\tilde{g}}$	721
$m_{\tilde{\chi}_2^\pm}$	536
$m_{\tilde{\chi}_1^\pm}$	229
$m_{\tilde{\chi}_4^0}$	536
$m_{\tilde{\chi}_3^0}$	525
$m_{\tilde{\chi}_2^0}$	229
$m_{\tilde{\chi}_1^0}$	120
$m_{\tilde{u}_L}$	684
$m_{\tilde{u}_R}$	664
$m_{\tilde{d}_L}$	688
$m_{\tilde{d}_R}$	663
$m_{\tilde{t}_2}$	682
$m_{\tilde{t}_1}$	437
$m_{\tilde{b}_2}$	682
$m_{\tilde{b}_1}$	663
$m_{\tilde{l}_L}$	281
$m_{\tilde{l}_R}$	232
$m_{\tilde{\tau}_2}$	291
$m_{\tilde{\tau}_1}$	224
$m_{\tilde{\nu}_2}$	281
$m_{\tilde{\nu}_1}$	108
$m_{H^\pm}$	561
m_H	555
m_A	555
m_h	114

When we simulate events that include this sequence of decays using Pythia, the chargino is decayed isotropically in its rest frame, and angular correlations between the lepton and jet are lost. Taking $\chi_1^\pm$ to be pure charged wino, which it nearly is for the chosen parameters, the squarks that can initiate this sequence are $\tilde{u}_L$, $\tilde{d}_L$, $\tilde{u}_L^*$, or $\tilde{d}_L^*$. If these are produced with equal abundance, then the quark-lepton angular correlations average out to zero, even if we focus on a particular sign for the charge of the lepton. In this case the fact that Pythia does not keep track of the angular correlations is not important, and the true m_{ql} distribution looks the same as the distribution for a 2-body/2-body sequence of decays with an intermediate scalar, shown as the dashed line of Fig. 4.

However, there is no reason to expect that $\tilde{u}_L$, $\tilde{d}_L$, $\tilde{u}_L^*$, and $\tilde{d}_L^*$ will be produced in equal abundance. For example, for the sample point chosen above, the dominant SUSY production is squark + gluino. The gluino decays with roughly equal probabilities to all four of these possibilities, but the parton distribution functions dictate that the squark produced is less likely to be $\tilde{d}_L$ than $\tilde{u}_L$, and less likely still to be an antisquark. The sequence $\tilde{u}_L \to (\chi^+)d \to (\tilde{\nu}_1 l^+)d$ gives a quark and a lepton with opposite helicities, while the sequence $\tilde{d}_L \to (\chi^-)u \to (\tilde{\nu}_1^* l^-)u$ gives a quark and lepton with the same helicity. So, the jet and lepton tend to be more back-to-back when produced by $\tilde{d}_L$, and more in the same direction when produced by $\tilde{u}_L$. Given that $\tilde{u}_L$ is produced more abundantly than $\tilde{d}_L$, we should then expect that the combined m_{ql} distribution will look somewhat softer than the dashed line of Fig. 4, without the sharp edge. On the other hand, if we focus on jet-l^- invariant-masses, then we should expect distribution to be even harder than for the case without angular correlations. This is because l^- is produced in the sequences beginning with $\tilde{d}_L$ (which gives a quark and a lepton with the same helicity) or with $\tilde{u}_L^*$ (which gives an antiquark and a lepton with the opposite helicity). Assuming $\tilde{d}_L$ is produced more abundantly than $\tilde{u}_L^*$, the jets and leptons will then tend to be more back-to-back on average.

Although these angular-correlation issues are important, we set them aside in what follows. The jet-lepton kinematic edge we identify below may be softened when both signs of lepton charge are allowed, but by requiring negatively charged leptons, an even harder distribution should result.

For the parameter point chosen above, we find a total SUSY production cross section of 20.4 pb. We generate $\sim$160 000 events, corresponding to $\sim 8\ \text{fb}^{-1}$, and keep events with the following characteristics:

(i) Exactly two jets with $p_T > 150$ GeV.
(ii) Exactly one isolated lepton with $p_T > 10$ GeV.
(iii) A transverse mass $m_T > 250$ GeV.
(iv) Missing transverse energy $\not{E}_T > 250$ GeV.

We find that the number of $t\bar{t}$ events passing these cuts is more than a factor of 20 smaller than that from SUSY production. Using Alpgen 2.12 [51], we estimate the $W +$ jets background by obtaining $W + 2$ jet events with a generator-level cut on the two jets, $p_T > 100$ GeV. We find that this source of background is even more suppressed than the $t\bar{t}$ background.

In Fig. 10 we show the jet-lepton invariant-mass distribution for the SUSY events, where for each event we include the two invariant masses obtained by pairing the isolated lepton with both of the hard jets. A fairly steep drop-off in this distribution is seen near the expected kinematic end point, which is at 568 GeV. There is a large combinatorial background associated with incorrect lepton-jet pairings, whose shape one can attempt to guess by looking at the invariant-mass distribution for lepton-jet pairings from different events. A similar method is used to study SUSY ditau signatures in [52], for example. Whether the distribution for incorrect lepton-jet pairings from the same event and the distribution for lepton-jet pairings from different events are similar should obviously depend on the

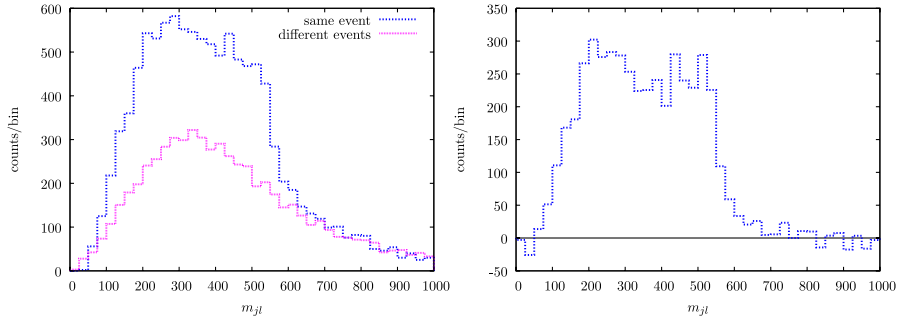

FIG. 10 (color online). Left: invariant-mass distribution for jets and leptons in the same event, and rescaled invariant-mass distribution for jets and leptons in different events. Right: the subtracted distribution.

strength of the correlations in the momenta of incorrectly paired jets and leptons from the same event. Because the squarks will tend to be at least somewhat back-to-back, one would expect correlations at some level. However, in the present example, the shape of the distribution for lepton-jet pairings from different events matches rather well with the shape of the same-event distribution beyond the expected kinematic end point. Rescaling the different-events distribution to match the same-event distribution at high invariant mass, and then subtracting that rescaled distribution off, the drop-off near the kinematic end point becomes clearer, as shown in the second plot of Fig. 10. The bump in the distribution at relatively low invariant mass ($m_{jl} \lesssim$ 300 GeV) is due to cascades involving $\tilde{t}_1$.

A jet-lepton invariant-mass distribution of the sort shown can also arise without mixing, from production of ordinary sneutrinos. Furthermore, a jet-lepton signal can be produced in other ways in the MSSM. A first example, relevant if the decay $\tilde{\chi}_1^- \to \tilde{\chi}_1^0 W^-$ is dominant, is given by the sequence $\tilde{q} \to (\tilde{\chi}_1^-)q \to (\tilde{\chi}_1^0 W^-)q$, with W^- decaying leptonically. A second example is given by the decay sequence $\tilde{q} \to (\tilde{\chi}_1^-)q \to ([\tilde{l}_L]\bar{\nu})q \to ([\tilde{\chi}_1^0 l]\bar{\nu})q$. In both of these examples, the lepton and jet are accompanied by a neutrino, and so the kinematics are different than in the case of sneutrino production. One would expect the jet-lepton invariant-mass distributions to reflect these differences at some level. In fact, for the second example one can show that the distribution is softer than for a 2-body/2-body sequence with an intermediate scalar, regardless of the sign of the lepton considered. The analysis for the first example is more complex, as there is no intermediate scalar in the decay chain, but here there are other things to go on as well. For example, one could look for events where the decay $\tilde{\chi}_1^\pm \to \tilde{\chi}_1^0 W^\pm$ occurs on both sides of the event, with one W decaying leptonically and the other hadronically. If a significant number of hadronic W's were reconstructed by looking for events of this type, the $\tilde{\chi}_1^\pm \to \tilde{\chi}_1^0 W^\pm$ interpretation would have to be favored over the $\chi^\pm \to \tilde{\nu}_1 l$ interpretation. Another potentially important difference is that one has flavor universality for the decays $W^- \to l\bar{\nu}$, but not necessarily for the decays $\chi^- \to \tilde{\nu}_1^* l$.

Other observables may be useful for distinguishing production of mixed -sneutrinos and ordinary sneutrinos. For example, for the parameter point considered above, χ_2^0 decays invisibly, and the flavor-subtracted OSSF dilepton invariant-mass distribution has no particularly distinctive features. On the MSSM side, for much of the parameter space for which $\tilde{\chi}_1^- \to \tilde{\nu}^* l$ occurs, $\tilde{\chi}_2^0 \to \tilde{l}_L^* l$ also occurs, giving rise to an OSSF dilepton signature upon the subsequent decay $\tilde{l}_L^* \to \tilde{\chi}_1^0 l^+$. These decays tend to come along with each other because in the MSSM the masses of $\tilde{\nu}$ and $\tilde{l}_L$ are split only by electroweak symmetry breaking,

$$m_{\tilde{l}_L}^2 - m_{\tilde{\nu}}^2 \leq m_W^2. \tag{22}$$

Provided that $m_{\tilde{\chi}_1^\pm}$ is not much larger than $m_{\tilde{\chi}_2^0}$, the decay $\tilde{\chi}_2^0 \to \tilde{l}_L^* l$ thus tends to be kinematically accessible when $\tilde{\chi}_1^- \to \tilde{\nu}^* l$ is. The essential point is that, because the mass of the mixed sneutrino is not directly linked to the mass of the charged slepton, it is easier than in the MSSM to have signals for sneutrino production in the absence of signals for charged slepton production.

One way to have $\tilde{\chi}_1^- \to \tilde{\nu}^* l$ without $\tilde{\chi}_2^0 \to \tilde{l}_L^* l$ in the MSSM is to have a closely spaced spectrum with $m_{\tilde{\nu}} < m_{\tilde{\chi}_1^\pm}$ and $m_{\tilde{l}_L} > m_{\tilde{\chi}_2^0}$. Mass measurements would clearly be helpful in distinguishing a mixed-sneutrino scenario from this MSSM one. For example, if it were established that the sneutrino-chargino mass splitting were quite large, it would disfavor the MSSM scenario just described.

Mass Estimation

Here we consider how the technique proposed by [50] can be used to probe the mass spectrum. The authors of that paper consider a general situation in which the sequence $Y \to lX$ and $X \to l'N$ occurs on both sides of an event. The particle N is invisible, so the final-state topology involves four leptons and missing energy. A typical SUSY example of this situation has $Y = \tilde{\chi}_2^0$, $X = \tilde{l}$, and $N = \tilde{\chi}_1^0$. For the mixed-sneutrino scenario considered in this section, we have a large number of events with $\tilde{q} \to \chi^\pm q \to \tilde{\nu} l q$ on either side. The event topology is thus quite similar, but with two of the four leptons replaced with quarks.

For a set of candidate values for the unknown masses m_Y, m_X, m_N, one can check whether the observed kinematics of a given event of this type are consistent with those values. The procedure of [50] is to fix two of the masses and keep track of the number of allowed events as the third mass is scanned. A candidate value for the third mass is identified by looking for a dramatic feature in the resulting distribution, e.g. a sharp drop or peak in the number of allowed events. In our implementation we apply a smoothing procedure to the events distribution and identify the candidate mass as the point where the second derivative of the distribution is minimized.

These steps are then iterated—the third mass is fixed at its new candidate value while the first mass is scanned, and so on. It was found in [50] that this procedure does not converge, and it was suggested that the actual masses can be estimated as the ones that give a global peak in the number of consistent events as the iterations are performed. In our implementation we find that for some of the events samples the candidate masses quickly settle near a final value, while for others the candidate masses continue to jump around indefinitely. Even in the case where the candidate masses continue to jump around, they at least wind up in stable ''orbits'' after a sufficient number of iterations. We take the average values of these orbits as the mass estimates for a given event sample.

Although we do not find that our implementation of this procedure leads to a reliable estimate of the sneutrino mass, it does give a reliable estimate of the chargino-sneutrino mass splitting. We first apply the technique to the same parameter point described above, taking the most optimistic case where the chargino decays produce electrons and muons and not taus. We select events with exactly two jets with $p_T > 150$ GeV, and exactly two leptons with $p_T > 10$ GeV. The leptons are required to have the same sign in order to suppress standard model backgrounds. We find that the efficiencies for passing these cuts are 1.4% for the SUSY sample and 1.3×10^{-5} for the $t\bar{t}$ sample, giving a ratio of SUSY events to $t\bar{t}$ events of over 20. More problematic than the $t\bar{t}$ background is the background from SUSY events in which the selected jets and leptons do not come from the desired decay chains. Using 12 sets of 1000 events, we obtain 12 estimates for $(m_{\tilde{q}}, m_{\tilde{\chi}_1^\pm}, m_{\tilde{\nu}_1})$. Combined, these event samples correspond to an integrated luminosity of roughly 42 fb^{-1}. For each event sample, we take the average values of the candidate masses at large iteration number as the mass estimates for that sample. Averaging *these* estimates gives

$$(m_{\tilde{q}}, m_{\tilde{\chi}_1^\pm}, m_{\tilde{\nu}_1}) = (688 \pm 33 \text{ GeV}, 239 \pm 27 \text{ GeV}, 110 \pm 30 \text{ GeV}), \qquad m_{\tilde{\chi}_1^\pm} - m_{\tilde{\nu}_1} = 129 \pm 7 \text{ GeV},$$

compared with the actual values, $(m_{\tilde{q}}, m_{\tilde{\chi}_1^\pm}, m_{\tilde{\nu}_1}) = (684\text{–}688 \text{ GeV}, 229 \text{ GeV}, 108 \text{ GeV})$ and $m_{\tilde{\chi}_1^\pm} - m_{\tilde{\nu}_1} = 121$ GeV. If the chargino decays produce e, μ, and τ with the same probability, the resolution worsens somewhat. Performing the same procedure on 10 sets of 1000 events, we obtain

$$(m_{\tilde{q}}, m_{\tilde{\chi}_1^\pm}, m_{\tilde{\nu}_1}) = (720 \pm 40 \text{ GeV}, 263 \pm 35 \text{ GeV}, 140 \pm 42 \text{ GeV}), \qquad m_{\tilde{\chi}_1^\pm} - m_{\tilde{\nu}_1} = 123 \pm 10 \text{ GeV}.$$

If we now redo the same analysis with the same parameters except with the sneutrino mass increased to 142 GeV, we obtain $m_{\tilde{\nu}_1} = 116 \pm 22$ GeV and $m_{\tilde{\chi}_1^\pm} - m_{\tilde{\nu}_1} = 92 \pm 7$ GeV (versus an actual splitting of 87 GeV). Increasing the sneutrino mass further to 185 GeV gives $m_{\tilde{\nu}_1} = 124 \pm 23$ GeV and $m_{\tilde{\chi}_1^\pm} - m_{\tilde{\nu}_1} = 48 \pm 2$ GeV (versus an actual splitting of 44 GeV).

These results show that although the sneutrino mass estimates do not follow the actual values closely, the estimates of the chargino-sneutrino mass splitting do. So, this analysis can be used to find evidence against a closely spaced spectrum of the type described above. A more sophisticated implementation of this mass-estimation method, or different methods such as those proposed in [53,54] may do a better job at estimating the sneutrino mass itself.

C. Associated production of Z/h with a lepton

For some regions of parameter space, the heavier sneutrino would be produced at the LHC. In particular, if a chargino with significant charged-wino component is heavier than the heavier sneutrino, it can decay to that sneutrino and a charged lepton. The question is then how the heavier sneutrino decays. One possibility is $\tilde{\nu}_2 \to \tilde{\chi}_1^0 \nu$, which is just what one might expect in the MSSM. Here we consider a more distinctive scenario, in which the splitting with the lighter sneutrino and the sneutrino mixing angle are both large enough that the branching ratios for $\tilde{\nu}_2 \to \tilde{\nu}_1 Z$ and $\tilde{\nu}_2 \to \tilde{\nu}_1 h$ are both significant. In this case we find

(i) Cascade production of Z bosons leads to a clean signature if the sneutrino contains e or μ flavor. The shape of the trilepton invariant-mass distribution can in principle distinguish this signature from MSSM signatures involving Z bosons.

(ii) If the sneutrino is dominantly τ flavored, a much larger integrated luminosity of the LHC is necessary to see cascade Z production

(iii) Cascade production of Higgs bosons can also lead to distinctive signatures, both through the $h \to b\bar{b}$ and $h \to \gamma\gamma$ decay channels.

As an example of a point in parameter space with these interesting heavy-sneutrino decays, consider the weak-scale values shown in Table III, and the resulting mass spectrum of Table IV. We find that the SUSY production

TABLE III. Parameters chosen to study $\tilde{\nu}_2 \to \tilde{\nu}_1 Z$ and $\tilde{\nu}_2 \to \tilde{\nu}_1 h$ signatures. All masses are in GeV.

$\tan\beta$	μ	m_A	M_1	M_2	M_3	A_t	$A_{b,\tau}$	$\tilde{m}^2_{Q,u,d}$	$\tilde{m}^2_L$	$\tilde{m}^2_e$	$m_{\tilde{\nu}_1}$	θ
10	600	350	200	500	700	−800	0	$(600)^2$	$(300)^2$	$(250)^2$	82	0.2

cross section for this spectrum is 24 pb, and the relevant branching ratios for the signals that interest us here are $Br(\chi_1^+ \to \tilde{\nu}_2 l) = 32\%$ $(l = e, \mu)$, $Br(\tilde{\nu}_2 \to \tilde{\nu}_1 Z) = 37\%$, and $Br(\tilde{\nu}_2 \to \tilde{\nu}_1 h) = 37\%$. These decays lead to a trilepton signature for the case of Z production, and $lb\bar{b}$ and $l\gamma\gamma$ signatures for the case of Higgs production.

To explore these signatures, we generate 640 k SUSY events, corresponding to about 27 fb^{-1} of integrated luminosity. We select events with the following properties to study the lepton-Z signature:

(i) Three isolated leptons with $p_T > 10$ GeV. Two of these must be of opposite sign and same flavor, with $|m_{l^+l^-} - m_Z| < 10$ GeV.

TABLE IV. Superpartner and Higgs boson masses for the parameter point of Table III.

$m_{\tilde{g}}$	721
$m_{\tilde{\chi}_2^\pm}$	629
$m_{\tilde{\chi}_1^\pm}$	474
$m_{\tilde{\chi}_4^0}$	630
$m_{\tilde{\chi}_3^0}$	601
$m_{\tilde{\chi}_2^0}$	474
$m_{\tilde{\chi}_1^0}$	196
$m_{\tilde{u}_L}$	623
$m_{\tilde{u}_R}$	624
$m_{\tilde{d}_L}$	628
$m_{\tilde{d}_R}$	626
$m_{\tilde{t}_2}$	734
$m_{\tilde{t}_1}$	524
$m_{\tilde{b}_2}$	639
$m_{\tilde{b}_1}$	615
$m_{\tilde{l}_L}$	303
$m_{\tilde{l}_R}$	254
$m_{\tilde{\tau}_2}$	309
$m_{\tilde{\tau}_1}$	249
$m_{\tilde{\nu}_2}$	299
$m_{\tilde{\nu}_1}$	82
$m_{H^\pm}$	359
m_H	351
m_A	351
m_h	114

(ii) $m_T > 100$ GeV, where m_T is the transverse mass constructed from the momentum of the third lepton and the missing p_T.

(iii) $\sum p_T > 800$ GeV, where the sum is over jets with $p_T > 20$ GeV, leptons and photons with $p_T > 10$ GeV, and missing p_T.

These cuts select 1058 SUSY events. We find that the backgrounds from $t\bar{t}$ (generated using Pythia) and from WZ, ZZ, and WW production (generated using Alpgen) are negligible by comparison. The trilepton invariant-mass distribution for events passing the cuts is shown in the first plot of Fig. 11. The distribution shows a steep drop-off near the expected end point at 364 GeV. Along the lines of what was done for the jet-lepton mass distribution, one can attempt to subtract off the SUSY background by guessing that the shape of the SUSY background contribution to the distribution should be similar to the distribution obtained by matching the Z candidates from one event with leptons from different events. Subtracting off this distribution gives the distribution shown in the second plot of Fig. 11. A lower kinematic end point should in principle be observed at around 148 GeV. With greater statistics it is possible that a second edge near this value would become clear in the subtracted distribution.

Z bosons can also be produced in association with leptons in the MSSM, in processes such as $\tilde{\chi}_2^- \to (\tilde{\chi}_1^-)Z \to (\tilde{\nu}^* l)Z$. In principle, this MSSM process is distinguishable from the mixed-sneutrino signature considered above by examining the Z- l invariant-mass distribution. In the mixed-sneutrino case, the intermediate $\tilde{\nu}_2$ decays isotropically in its rest frame. The amplitude-squared for the chargino decay into $\tilde{\nu}_1 lZ$ is thus constant, and the m_{Zl} distribution is trapezoidal, rising linearly between lower and upper kinematic edges. In the MSSM sequence $\tilde{\chi}_2^- \to (\tilde{\chi}_1^-)Z \to (\tilde{\nu}^* l)Z$, there is no intermediate scalar, and there will generically be some dependence of the amplitude-squared on m_{Zl}. The chargino-chargino- Z coupling can be written as

$$\bar{\chi}_2^- \gamma^\mu (c_L P_L + c_R P_R) \chi_1^-, \tag{23}$$

where the couplings c_L and c_R are determined by the mixing in the chargino sector. These couplings are typically not equal. In the narrow-width approximation, the amplitude-squared for the decay $\tilde{\chi}_2^- \to \tilde{\nu}^* lZ$ takes the form $\alpha + \beta(|c_L|^2 - |c_R|^2) m_{lZ}^2$, where α and β are constants. Provided the chargino-Z coupling is indeed chiral, the invariant-mass distributions thus differ in the MSSM and mixed-sneutrino cases. A similar issue was raised in

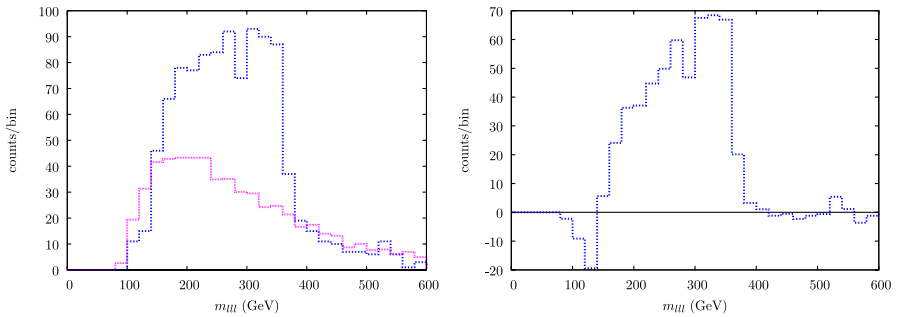

FIG. 11 (color online). Left: invariant-mass distribution for trileptons in the same event, and rescaled invariant-mass distribution for Z candidates and leptons in different events. Right: the subtracted distribution.

considering the possible production of Z bosons in top-squark decays in [55].

If only the $\tilde{\nu}_\tau$ mixes with a sterile neutrino, the signature becomes much less clean than what we have considered. In this case $\tilde{\nu}_{e,\mu}$ decay straight to $\tilde{\chi}_1^0\nu$, and so one is forced to look for signals from associated $\tau - Z$ production. To explore these we use a much larger sample of SUSY events corresponding to roughly 170 fb^{-1}, and impose the same cuts as before, except that his time we require a reconstructed τ and two opposite-sign, same-flavor leptons that reconstruct a Z. We also place a veto on b-tagged jets to help reduce the $t\bar{t}$ background. After these cuts, we are left with 1551 SUSY events. We estimate that the $t\bar{t}$ and WZ backgrounds give fewer events by factors of 8 and 30, respectively. In our plots we will not include these background contributions, as we have not generated a large enough $t\bar{t}$ sample; it is likely that more carefully chosen cuts can improve the quoted signal to background ratio.

In the first plot of Fig. 12 we show the τll invariant-mass distribution for events passing the cuts, along with the (rescaled) distribution obtained by matching Z candidates from one event with τ's from a different event. The second plot of the same figure shows the subtracted distribution, which does have a recognizable end point.

To study the lepton-Higgs signature, we first select events with the following characteristics:

(i) Two b-tagged jets with $p_T > 20$ GeV.
(ii) Exactly one isolated lepton with $p_T > 10$ GeV.
(iii) A transverse mass $m_T > 200$ GeV.
(iv) Missing transverse energy $\not{E}_T > 200$ GeV.
(v) $\sum p_T > 800$ GeV, where the sum is over jets with $p_T > 20$ GeV, leptons and photons with $p_T > 10$ GeV, and missing p_T.

Working with the same 27 fb^{-1} sample used to analyze the lepton-Z signature, a total of 2432 SUSY events survive these cuts, a factor of 8 larger than the number of $t\bar{t}$ events that survive. The invariant-mass distribution for events passing these cuts is shown in the first plot of Fig. 13. A peak, although not a clean one, is evident at around 100 GeV, somewhat below the actual Higgs mass of 114 GeV. We keep events with $|m_{bb} - 100\ \text{GeV}| < 20$ GeV, and the m_{bbl} invariant-mass distribution for those events is shown in the second plot of Fig. 13. The distribution shows a significant drop-off near the expected end point, at 369 GeV.

For the parameter point chosen, the rate of Higgs production is large enough that the Higgs can also be seen through its decays to photons. For this analysis, we impose the same cuts as for the bbl analysis, except that we require two photons with $p_T > 10$ GeV instead of two b-tagged jets. A total of 60 SUSY events pass these cuts. We have checked that the backgrounds from $t\bar{t}$ production and $W\gamma\gamma$ + jets (estimated using Alpgen) are negligible. (In fact, it is possible that it would be advantageous to relax the kinematic cuts.) The $\gamma\gamma$ invariant-mass distribution for events passing these cuts is shown in the first plot of

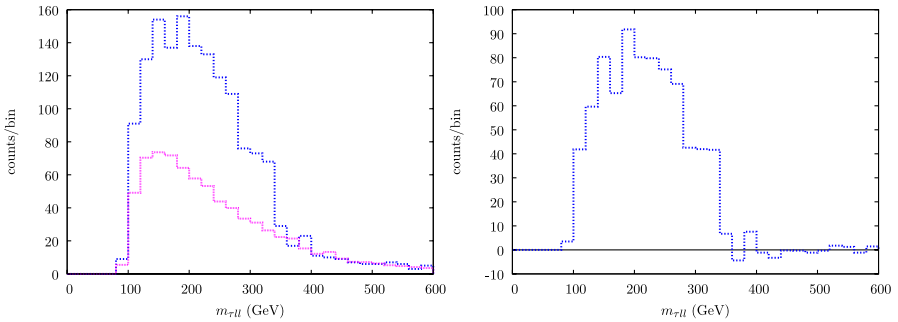

FIG. 12 (color online). Left: τll invariant-mass distribution for τ's and Z candidates in the same event, and rescaled invariant-mass distribution for τ's and Z candidates in different events. Right: the subtracted distribution.

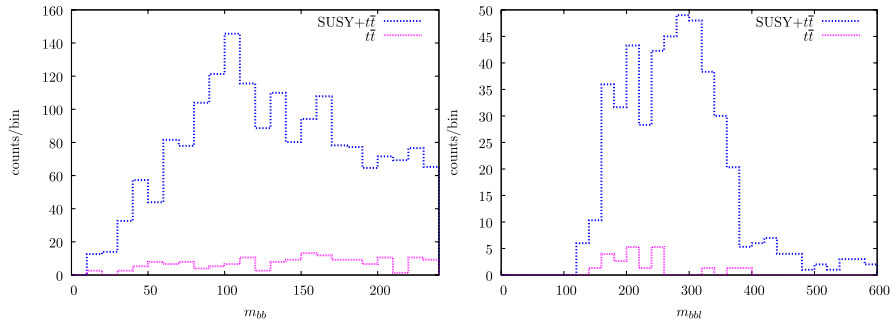

FIG. 13 (color online). Left: invariant-mass distribution for pairs of b-tagged jets. Right: for events in the peak of the m_{bb} distribution, invariant-mass distribution obtained by pairing Higgs candidates and leptons.

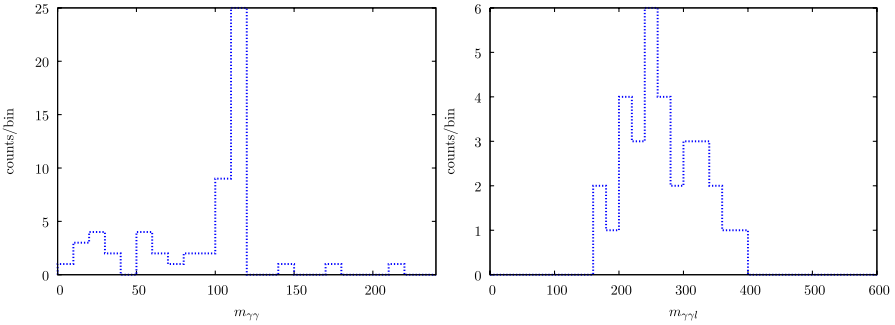

FIG. 14 (color online). Left: invariant-mass distribution for pairs of photons. Right: for events in the peak of the $m_{\gamma\gamma}$ distribution, invariant-mass distribution obtained by pairing Higgs candidates and leptons.

Fig. 14, and has an extremely clear peak. The $m_{\gamma\gamma l}$ distribution for events in this peak is shown in the second plot of Fig. 14; it falls below ~400 GeV as one would expect, but more statistics would be required to learn much from this distribution.

IV. CONCLUSIONS

In this paper we have explored the cosmology and collider phenomenology of mixed sneutrinos. Recent progress made by direct-detection experiments makes mixed-sneutrino dark matter quite constrained, but still viable. In the absence of lepton-number violation, parameter regions that give an appropriate relic abundance while evading direct-detection constraints include (1) light sneutrinos, $m_{\tilde{\nu}_1} < 10$ GeV, with relatively light gauginos and a rather large mixing angle, $\theta \sim 0.3$, (2) small mixing angles, $\theta \lesssim 0.07$, with $m_{\tilde{\nu}_1}$ near the Higgs funnel, or (3) small mixing angles with $m_{\tilde{\nu}_1}$ above threshold for annihilation to W pairs, for large values of heavier sneutrino masses, $m_{\tilde{\nu}_2} \gtrsim 500$ GeV.

Lepton-number violation in the sneutrino mass-sqaured matrix can suppress scattering of $\tilde{\nu}_1$ off of nuclei via Z exchange, making somewhat larger mixing angles viable. However, this lepton-number violation produces radiative contributions to neutrino mass. If the lepton-number violation is large enough to dramatically suppress the elastic scattering via Z exchange, the radiatively generated mass tends to approach or exceed the upper bound from cosmology. In principle one can suppress this radiatively generated neutrino mass by making the gauginos heavy, while still achieving a realistic relic abundance through annihilations mediated by Higgs and Z exchange, or by making the gauginos Dirac.

We have studied LHC signatures of mixed sneutrinos in general, without requiring the mixed sneutrino responsible for the signal to be the dark matter. If the mixed-sneutrino is the LSP, with a very small mixing angle, then the NLSP will typically be the only particle that decays to it with a large branching ratio. If this particle is the lightest neutralino, then the only effect of the mixed sneutrino is to alter the connection between collider physics and cosmology. If the NLSP is instead a right-handed slepton one expects an unusually large lepton multiplicity in the SUSY signal. Moreover, decays of the lightest neutralino can lead to an interesting opposite-sign, same-flavor (OSSF) dilepton signature. Since the dilepton signature arises from a two-body decay followed by a three-body decay, the shape of the dilepton invariant-mass distribution is significantly different from the sequence of two-body decays $\chi_2^0 \to (\tilde{l})l^+ \to (\chi_1^0 l^-)l^+$. It can also be distinguished from that arising from a three-body decay $\chi_2^0 \to \chi_1^0 l^+ l^-$, depending on factors such as the observed kinematic end point of the distribution. If the lightest neutralino decays to $\tilde{\tau}_1$ rather

than $\tilde{e}_R$ or $\tilde{\mu}_R$, the experimental signatures become more difficult to extract, but there is still the possibility of observing a large excess of events with taus produced in association with opposite-sign leptons, where the leptons come from W bosons produced in the decay $\tilde{\tau}_1 \rightarrow \tilde{\nu}_1 W$.

For larger mixing angles, it is possible that the mixed sneutrinos will be produced copiously at the LHC through chargino decays, or even from the decays of heavier sneutrinos. In the first case, the sequence $\tilde{q} \rightarrow (\chi^{\pm})q \rightarrow (\tilde{\nu}_1 l)q$ gives rise to a kinematic edge in the jet-lepton invariant-mass distribution. For broad regions of parameter space, not only $\rightarrow \chi^{\pm}$ but also $\tilde{\chi}_2^0$ decays dominantly to $\tilde{\nu}_1$, and in these regions the jet-lepton signature is present in the absence of an OSSF dilepton signature. This situation can also arise due to ordinary sneutrino production in the MSSM, but we have shown that mass-estimation methods may be helpful for distinguishing the mixed-sneutrino and MSSM scenarios, due to the fact that the sneutrino-charged slepton mass splitting is an electroweak symmetry breaking effect in the MSSM, but not in the mixed-sneutrino case.

Finally, if the predominantly left-handed sneutrinos $\tilde{\nu}_2$ are produced at the LHC, the decays $\tilde{\nu}_2 \rightarrow \tilde{\nu}_1 Z$ and $\tilde{\nu}_2 \rightarrow \tilde{\nu}_1 h$ may be important if kinematically accessible. Events with $\tilde{\nu}_2$ produced from chargino decay may then have Higgs or Z bosons produced in association with leptons. In this case, a distinctive $b\bar{b}l$ invariant-mass distribution can arise from Higgs production, and a distinctive trilepton invariant-mass distribution can arise from Z production. Because these decay chains feature an intermediate scalar, $\tilde{\nu}_2$, they can in principle be distinguished from MSSM decay chains such as $\tilde{\chi}_2^- \rightarrow (\tilde{\chi}_1^-)Z \rightarrow (\tilde{\nu}^* l)Z$, where the chargino-chargino- Z coupling is in general chiral. We leave a detailed analysis of this issue for future work.

ACKNOWLEDGMENTS

The work of Z. T. and D. T. S. was supported by NSF Grant No. 0555421 and by Research Corporation. N. W. was supported by NSF CAREER Grant No. PHY-0449818 and DOE Grant No. DE-FG02-06ER41417.

[1] M. W. Goodman and E. Witten, Phys. Rev. D **31**, 3059 (1985).
[2] T. Yanagida, in *Proceedings of the Workshop on the Unified Theory and Baryon Number in the Universe*, edited by O. Sawada and A. Sugamoto (KEK, Tsukuba, 1979).
[3] M. Gell-Mann, P. Ramond, and R. Slansky, in *Supergravity*, edited by F. Van Niewuwenhuizen and D. Freedman (North-Holland, Amsterdam, 1979), p. 315.
[4] N. Arkani-Hamed, L. J. Hall, H. Murayama, D. R. Smith, and N. Weiner, Phys. Rev. D **64**, 115011 (2001).
[5] N. Arkani-Hamed, L. J. Hall, H. Murayama, D. R. Smith, and N. Weiner, arXiv:hep-ph/0007001.
[6] F. Borzumati and Y. Nomura, Phys. Rev. D **64**, 053005 (2001).
[7] C. L. Chou, H. L. Lai, and C. P. Yuan, Phys. Lett. B **489**, 163 (2000).
[8] J. Angle *et al.* (XENON), Phys. Rev. Lett. **100**, 021303 (2008).
[9] C. Arina and N. Fornengo, J. High Energy Phys. 11 (2007) 029.
[10] L. Covi and S. Kraml, J. High Energy Phys. 08 (2007) 015.
[11] D. N. Spergel *et al.* (WMAP), Astrophys. J. Suppl. Ser. **170**, 377 (2007).
[12] D. S. Akerib *et al.* (CDMS), Phys. Rev. Lett. **96**, 011302 (2006).
[13] J. S. Hagelin, G. L. Kane, and S. Raby, Nucl. Phys. **B241**, 638 (1984).
[14] L. E. Ibanez, Phys. Lett. B **137**, 160 (1984).
[15] T. Falk, K. A. Olive, and M. Srednicki, Phys. Lett. B **339**, 248 (1994).
[16] L. J. Hall, T. Moroi, and H. Murayama, Phys. Lett. B **424**, 305 (1998).
[17] T. Asaka, K. Ishiwata, and T. Moroi, Phys. Rev. D **73**, 051301 (2006).
[18] S. Gopalakrishna, A. de Gouvea, and W. Porod, J. Cosmol. Astropart. Phys. 05 (2006) 005.
[19] H.-S. Lee, K. T. Matchev, and S. Nasri, Phys. Rev. D **76**, 041302 (2007).
[20] A. de Gouvea, S. Gopalakrishna, and W. Porod, J. High Energy Phys. 11 (2006) 050.
[21] S. K. Gupta, B. Mukhopadhyaya, and S. K. Rai, Phys. Rev. D **75**, 075007 (2007).
[22] G. Belanger, F. Boudjema, A. Pukhov, and A. Semenov, Comput. Phys. Commun. **176**, 367 (2007).
[23] A. Djouadi, J.-L. Kneur, and G. Moultaka, Comput. Phys. Commun. **176**, 426 (2007).
[24] R. Dermisek and J. F. Gunion, Phys. Rev. Lett. **95**, 041801 (2005).
[25] R. Dermisek and J. F. Gunion, Phys. Rev. D **73**, 111701 (2006).
[26] S. Chang, P. J. Fox, and N. Weiner, J. High Energy Phys. 08 (2006) 068.
[27] P. C. Schuster and N. Toro, arXiv:hep-ph/0512189.
[28] P. W. Graham, A. Pierce, and J. G. Wacker, arXiv:hep-ph/0605162.
[29] S. Chang, P. J. Fox, and N. Weiner, Phys. Rev. Lett. **98**, 111802 (2007).
[30] S. Chang and N. Weiner, arXiv:0710.4591.
[31] D. R. Smith and N. Weiner, Phys. Rev. D **64**, 043502 (2001).
[32] D. Tucker-Smith and N. Weiner, Phys. Rev. D **72**, 063509 (2005).

[33] H.-Y. Cheng, Phys. Lett. B **219**, 347 (1989).
[34] T. Hatsuda and T. Kunihiro, Nucl. Phys. **B387**, 715 (1992).
[35] M. A. Shifman, A. I. Vainshtein, and V. I. Zakharov, Phys. Lett. B **78**, 443 (1978).
[36] M. Tegmark *et al.*, Phys. Rev. D **74**, 123507 (2006).
[37] F. Governato *et al.*, Mon. Not. R. Astron. Soc. **374**, 1479 (2007).
[38] P. J. Fox, A. E. Nelson, and N. Weiner, J. High Energy Phys. 08 (2002) 035.
[39] G. Jungman, M. Kamionkowski, and K. Griest, Phys. Rep. **267**, 195 (1996).
[40] S. Desai *et al.* (Super-Kamiokande), Phys. Rev. D **70**, 083523 (2004).
[41] J. L. Feng, S.-f. Su, and F. Takayama, Phys. Rev. D **70**, 063514 (2004).
[42] J. L. Feng, S. Su, and F. Takayama, Phys. Rev. D **70**, 075019 (2004).
[43] A. Djouadi, M. M. Muhlleitner, and M. Spira, Acta Phys. Pol. B **38**, 635 (2007).
[44] T. Sjostrand, S. Mrenna, and P. Skands, J. High Energy Phys. 05 (2006) 026.
[45] The PGS simulation software is available at: http://www.physics.ucdavis.edu/conway/research/software/pgs/pgs4-general.htm.
[46] Prospino 2.0 is available at: http://www.ph.ed.ac.uk/tplehn/prospino/.
[47] W. Beenakker, R. Hopker, M. Spira, and P. M. Zerwas, Nucl. Phys. **B492**, 51 (1997).
[48] W. Beenakker, M. Kramer, T. Plehn, M. Spira, and P. M. Zerwas, Nucl. Phys. **B515**, 3 (1998).
[49] R. Bonciani, S. Catani, M. L. Mangano, and P. Nason, Nucl. Phys. **B529**, 424 (1998).
[50] H.-C. Cheng, J. F. Gunion, Z. Han, G. Marandella, and B. McElrath, J. High Energy Phys. 12 (2007) 076.
[51] M. L. Mangano, M. Moretti, F. Piccinini, R. Pittau, and A. D. Polosa, J. High Energy Phys. 07 (2003) 001.
[52] CMS Physics TDR, CERN/LHCC 2006-021.
[53] W. S. Cho, K. Choi, Y. G. Kim, and C. B. Park, arXiv:0709.0288.
[54] C. Lester and A. Barr, J. High Energy Phys. 12 (2007) 102.
[55] M. Perelstein and C. Spethmann, J. High Energy Phys. 04 (2007) 070.